

DTIC FILE COPY

AFOSR-TX- 88-1008

2

A NEW PROCESS FOR FINAL DENSIFICATION OF CERAMICS

FINAL REPORT

AD-A199 959

PROGRAM MANAGER: DR. DONALD ULRICH  
AIR FORCE OFFICE OF SCIENTIFIC RESEARCH

PRINCIPAL INVESTIGATOR: R. A. WAGNER  
BABCOCK & WILCOX

CONTRACTOR

BABCOCK & WILCOX  
a McDermott company

CONTRACT PERIOD

FEBRUARY 15, 1985 THRU MAY 14, 1988

DTIC  
SELECTE  
OCT 06 1988  
S & D

SPONSORED BY

ADVANCED RESEARCH PROJECTS AGENCY (DOD)  
ARPA ORDER NO. 5172  
PROGRAM CORD NO. 4D10  
MONITORED BY AFOSR UNDER CONTRACT NO. F49620-85-C-0053

88 10 5 308

Approved for public release;  
distribution unlimited.

LEGAL NOTICE

This report was prepared by Babcock & Wilcox (B&W), a McDermott company, as an account of work performed for the United States Government and neither the Government nor B&W, nor any person acting on their behalf:

(a) makes any warranty or representation, express or implied, with respect to the accuracy, completeness, or usefulness of the information contained in this report, or that the use of any information, apparatus, method, or process disclosed in this report may not infringe privately owned rights; or

(b) assumes any liabilities with respect to the use of, or for damages resulting from the use of, any information, apparatus, method, or process disclosed in this report.

DISCLAIMER

The views and conclusions contained in this document are those of the authors and should not be interpreted as necessarily representing the official policies, either expressed or implied, of the Defense Advanced Research Projects Agency or the U.S. Government.

Certification of Technical Data Conformity

The Contractor, Babcock & Wilcox, hereby certifies that, to the best of its knowledge and belief, the technical data delivered herewith under Contract No. F49620-85-C-0053 is complete, accurate, and complies with all requirements of the contract.

8/8/88

Date



N. F. Smith, Manager  
Contract Management Department  
Contract Research Division

## REPORT DOCUMENTATION PAGE

Form Approved  
OMB No. 0704-0188

1a. REPORT SECURITY CLASSIFICATION UNCLASSIFIED			1b. RESTRICTIVE MARKINGS		
2a. SECURITY CLASSIFICATION AUTHORITY			3. DISTRIBUTION / AVAILABILITY OF REPORT Approved for public release; Distribution is unlimited		
2b. DECLASSIFICATION / DOWNGRADING SCHEDULE			4. PERFORMING ORGANIZATION REPORT NUMBER(S)		
4. PERFORMING ORGANIZATION REPORT NUMBER(S)			5. MONITORING ORGANIZATION REPORT NUMBER(S) <b>AFOSR-TR- 88-1008</b>		
6a. NAME OF PERFORMING ORGANIZATION Babcock & Wilcox		6b. OFFICE SYMBOL (if applicable)	7a. NAME OF MONITORING ORGANIZATION AFOSR/NC		
6c. ADDRESS (City, State, and ZIP Code) 3315 Old Forest Road P.O. Box 10935 Lynchburg VA 24506-0935			7b. ADDRESS (City, State, and ZIP Code) Building 410 Bolling AFB, DC 20332-6448		
8a. NAME OF FUNDING / SPONSORING ORGANIZATION AFOSR		8b. OFFICE SYMBOL (if applicable) NC	9. PROCUREMENT INSTRUMENT IDENTIFICATION NUMBER F49620-85-C-0053		
8c. ADDRESS (City, State, and ZIP Code) Building 410 Bolling AFB, DC 20332-6448			10. SOURCE OF FUNDING NUMBERS		
			PROGRAM ELEMENT NO. 61102F	PROJECT NO. 2303	TASK NO. A3
11. TITLE (Include Security Classification) A New Process for Final Densification of Ceramics					
12. PERSONAL AUTHOR(S) R. A. Wagner					
13a. TYPE OF REPORT FINAL		13b. TIME COVERED FROM 2/85 TO 3/88		14. DATE OF REPORT (Year, Month, Day)	15. PAGE COUNT 62
16. SUPPLEMENTARY NOTATION					
17. COSATI CODES			18. SUBJECT TERMS (Continue on reverse if necessary and identify by block number)		
FIELD	GROUP	SUB-GROUP			
19. ABSTRACT (Continue on reverse if necessary and identify by block number)  See reverse					
20. DISTRIBUTION / AVAILABILITY OF ABSTRACT <input checked="" type="checkbox"/> UNCLASSIFIED/UNLIMITED <input type="checkbox"/> SAME AS RPT. <input type="checkbox"/> DTIC USERS			21. ABSTRACT SECURITY CLASSIFICATION UNCLASSIFIED		
22a. NAME OF RESPONSIBLE INDIVIDUAL Dr. Donald R. Ulrich			22b. TELEPHONE (Include Area Code) (202) 767-4963	22c. OFFICE SYMBOL NC	

The objective of this program was to demonstrate the feasibility of a novel densification process based on supercritical fluids. Using this process carbon/carbon composites were impregnated with silicon carbide precursors and pyrolyzed to produce oxidation resistant pore coatings. The resulting samples were characterized in terms of silicon distribution, mechanical properties, and oxidation resistance.

The solubility behavior of candidate carbon and silicon carbide precursors was determined in supercritical propane and carbon dioxide. In addition, two silicon carbide precursors were fractionated and characterized to establish the molecular weight dependence of the char yield. The results of the solubility and fractionation studies were then used to guide the impregnation program. 1525 ←

Characterization results demonstrated that significant depositions of silicon carbide precursor were achieved in both macro and microporous regions of carbon/carbon composites. As a result of SCF impregnations the bend strength increased by 47 percent and the oxidation rate decreased by almost an order of magnitude in the 500 to 600°C temperature range. The stressed oxidation results also demonstrate the increased oxidation resistance of impregnated samples at 593°C.

Supercritical fluids were also used to coat fibers with a silicon carbide precursor in a demonstration of their potential to control the fiber/matrix interface of composites.

Finally, supercritical fluid fractionation was shown to be a viable method of controlling the physical properties and char yields of silicon carbide precursors.

A NEW PROCESS FOR FINAL DENSIFICATION OF CERAMICS

FINAL REPORT

PROGRAM MANAGER: DR. DONALD ULRICH  
AIR FORCE OFFICE OF SCIENTIFIC RESEARCH

PRINCIPAL INVESTIGATOR: R. A. WAGNER  
BABCOCK & WILCOX

CONTRACTOR

BABCOCK & WILCOX  
a McDermott company

CONTRACT PERIOD

FEBRUARY 15, 1985 THRU MAY 14, 1988

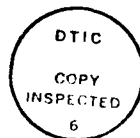
SPONSORED BY

ADVANCED RESEARCH PROJECTS AGENCY (DOD)  
ARPA ORDER NO. 5172  
PROGRAM CORD NO. 4D10  
MONITORED BY AFOSR UNDER CONTRACT NO. F49620-85-C-0053

FOREWORD

This report was prepared by the Research and Development Division of Babcock and Wilcox, Lynchburg, Virginia, and describes work performed under Contract F49620-85-C-0053, "A New Process For Final Densification of Ceramics", for the period February 15, 1985 through May 14, 1988. This work was jointly sponsored by the Advanced Research Projects Agency (DOD) ARPA order number 5172 program CORD NO. 4D10 and AFOSR. The program was administered under the direction of the Chemical Structures Division, Directorate of Chemical and Atmospheric Sciences, Air Force Office of Scientific Research, Bolling Air Force Base, Washington, D.C. 20332-6448. The program managers were Dr. Kay Rhyne and Major Steve Wax, DARPA and Dr. Donald Ulrich, AFOSR.

Dr. R. A. Wagner was the B&W principal investigator and final program manager. Mr. D. R. Petrak was the B&W program manager for the initial portion of the program. Dr. V. J. Krukonis and Mr. M. Coffey, PHASEX Corporation, were responsible for the supercritical fluid processing. The contributions of the following B&W personnel are acknowledged: Mr. J. M. Smith (supercritical fluid processing and sample characterization), Mr. N. W. White (SEM characterization), and Mr. J. H. Worley (mechanical testing).



SEARCHED	INDEXED
SERIALIZED	FILED
APR 1988	
FBI - MEMPHIS	
A-1	

## LIST OF ILLUSTRATIONS

FIGURE		PAGE
1	Summary of Program Results	3
2	Generalized P-T Phase Diagram For Single Component System Showing Supercritical (SCF) Regime	5
3	Solubility of Two Organic Compounds in Supercritical Fluids	8
4	Solubility of Naphthalene in CO <sub>2</sub>	10
5	Schematic Diagram of a Supercritical Fluid Extraction Process	11
6	Impregnation Processing Flow Diagram	14
7	Polymer Processing Flow Diagram	15
8	Experimental Apparatus for Supercritical Fluid Extraction and Impregnation	19
9	Impregnation Cycle Process Data	21
10	Schematic Diagram of Constant Composition View Cell	23
11	Solubility of Polycarbosilane	25
12	View Cell Solubility/Precipitation Sequence	28
13	View Cell Deposit and Rapid Precipitation Result	30
14	GPC Results for Two Lots of Polycarbosilane	32
15	Polycarbosilane 1000°C Char Yield	34

16	UCPS 1000°C Char Yield	35
17	ACC2 Impregnation Weight Gain	37
18	ACC2 Impregnation Density Change	38
19	ACC2 Impregnation Porosity Change	39
20	3D Carbon/Carbon Density Change	41
21	SCF Fiber Coating Microstructure	42
22	510°C Oxidation Results	44
23	538°C Oxidation Weight Loss	45
24	593°C Oxidation Results	46
25	593°C Stressed Oxidation Results	47
26	Oxidation Rate of As Received and SCF Impregnated ACC2	49
27	As Received and SCF Impregnated ACC2 Microstructures	50
28	SiC Concentration in ACC2	51
29	SiC Filled Weave Intersections and Fiber/Matrix Interface In ACC2	52
30	Cross Section of SCF Impregnated 3D C/C	53
31	SiC Accumulation at Tow Bundle Interface	54
32	SiC Filled Tow Bundle Crack	56



LIST OF TABLES

	PAGE
1 Critical Point Conditions for Common Gases	6
2 Comparison of Properties of Supercritical Fluids and Organic Solvents	7
3 Carbon and Silicon Carbide Precursors	17
4 Solubility Results for SC1008 Phenolic Resin	26
5 Solubility Results for FURCARB	26
6 Solubility Results for 15 Vacuum Coal Tar Pitch	27
7 UC Polysilane Fractionation Results	33

## 1.0 EXECUTIVE SUMMARY

The objective of this program was to demonstrate the feasibility of a novel densification process based on supercritical fluids. The definition and attributes of supercritical fluids are shown in Figure 1A. Using this process carbon/carbon composites were impregnated with silicon carbide precursors and pyrolyzed to produce oxidation resistant pore coatings. The resulting samples were characterized in terms of silicon distribution, mechanical properties, and oxidation resistance.

The solubility behavior of candidate carbon and silicon carbide precursors was determined in supercritical propane and carbon dioxide. In addition, two silicon carbide precursors were fractionated and characterized to establish the molecular weight dependence of the char yield. The results of the solubility and fractionation studies were then used to guide the impregnation program.

Characterization results summarized in Figure 1B, 1C, 1D, 1E, and 1F, demonstrated that significant depositions of silicon carbide precursor were achieved in both macro and microporous regions of carbon/carbon composites as shown in Figures 1B and 1C respectively. As a result of SCF impregnations the bend strength increased by 47 percent and the oxidation rate decreased by almost an order of magnitude in the 500 to 600°C temperature range, Figure 1D. The stressed oxidation results shown in Figure 1E also demonstrate the increased oxidation resistance of impregnated samples at 593°C.

Supercritical fluids were also used to coat fibers with a silicon carbide precursor in a demonstration of their potential to control the fiber/matrix interface of composites as shown in Figure 1F.

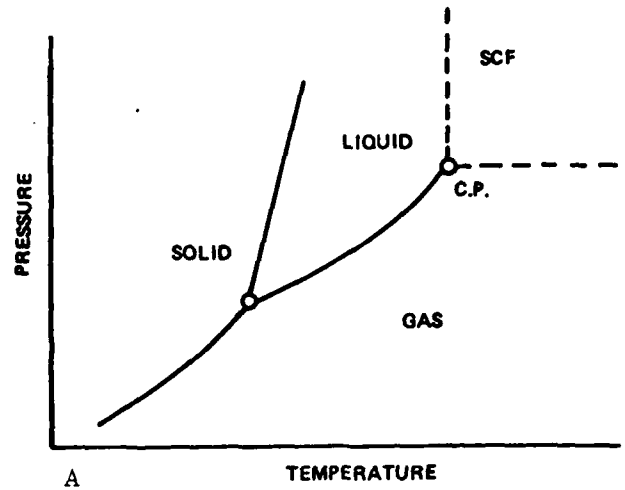
Finally, supercritical fluid fractionation was shown to be a viable method of controlling the physical properties and char yields of silicon carbide precursors.

Although several significant accomplishments of SCF processing were demonstrated, much work remains to be done. In the area of oxidation protection of carbon/carbon composites future work needs to focus on chemistries beyond

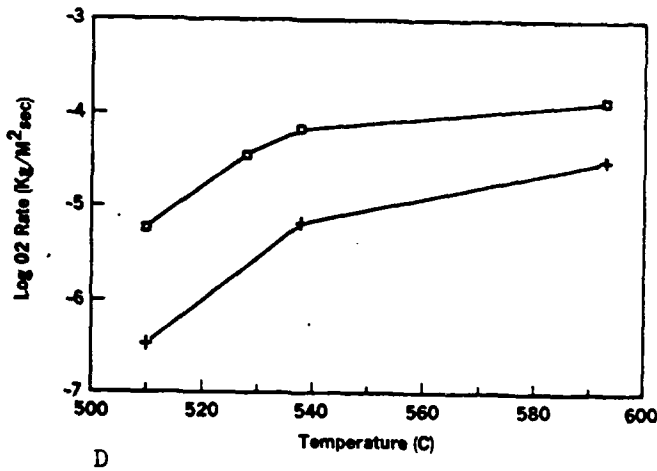
silicon carbide to develop glass forming systems designed to flow and seal cracks and pores. Further, the SCF developed pore coatings need to be integrated with state of the art coatings and sealers to optimize the overall oxidation protection system.

### SUPERCRITICAL FLUIDS

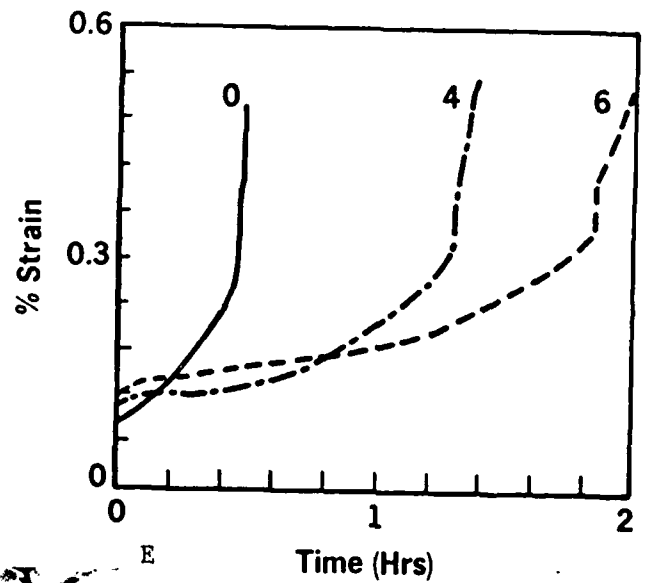
- MANY GASES EXHIBIT ENHANCED SOLVENT POWER ABOVE THE CRITICAL POINT
- CRITICAL POINT FOR MANY GASES OF INTEREST ARE AT LOW TEMPERATURES AND MODERATE PRESSURES, E.G., CO<sub>2</sub>, 31°C, 73 ATM.
- GASES HAVE LOW VISCOSITY AND NO SURFACE TENSION, THEREFORE CAN PENETRATE FINE POROSITY
- SOLUTION ↔ PRECIPITATION CAN BE CONTROLLED BY CHANGES IN PRESSURE OR TEMPERATURE
- SCF IS ATTRACTIVE FOR BOTH EXTRACTION AND IMPREGNATION PROCESSES



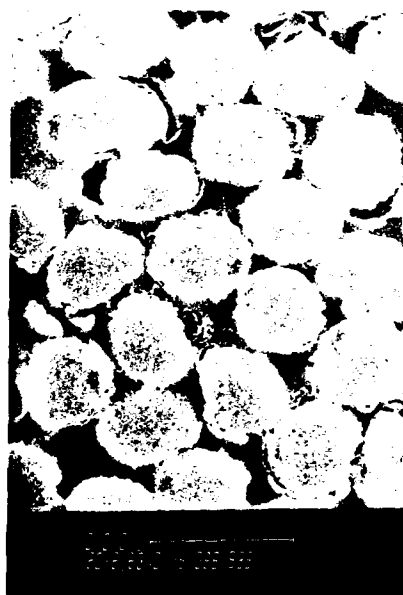
### Oxidation Rate of ACC2



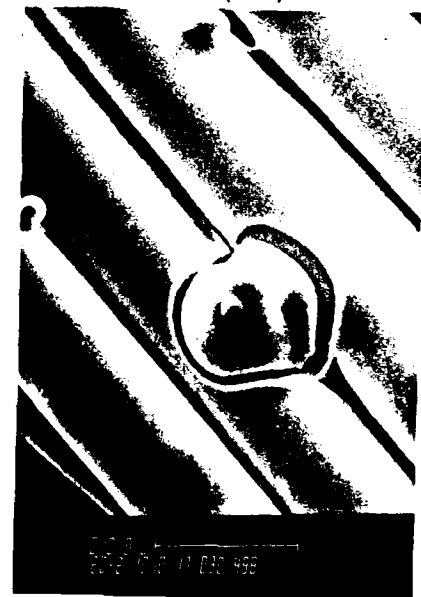
### Stressed Oxidation



B



C



F

FIGURE 1 SUMMARY OF PROGRAM RESULTS •

## 2.0 INTRODUCTION

Increasing utilization of carbon/carbon (C/C) composites in oxidizing atmospheres has resulted in a variety of oxidation protection systems designed to maintain the excellent mechanical properties of these materials. A cross section of a typical system consists of a glassy seal coat, a CVD or pack cementation SiC or Si<sub>3</sub>N<sub>4</sub> coat, and finally the carbon/carbon substrate with particulate inhibitors and pore coating.

The CVD or pack cementation SiC coating provides the primary protection layer but cracks caused by differential thermal expansion between the coating and substrate allow oxygen penetration to the C/C substrate. At temperatures over 650°C, the glassy seal coat flows to heal cracks and current approaches provide acceptable protection. However, active oxidation of carbon starts at about 400°C and other approaches are required to prevent oxidation between 400°C and 600°C.

Because the substrate is accessible through the coating cracks, some form of matrix inhibition is necessary to limit oxidation of the substrate. Glass forming particulates added to the substrate have been reported<sup>1</sup> to improve the oxidation resistance by reacting with oxygen and expanding to fill and seal the crack with glass. Other investigators<sup>2</sup> have applied sol-gel derived pore coatings to protect the substrate until surface cracks close or heal.

The approach taken in this program utilized the unique transport properties and pressure dependent solubility of supercritical fluids to develop an oxidation resistant pore coating in advanced carbon/carbon composites. Polycarbosilane was used as a model precursor to demonstrate the feasibility of this concept. Following multiple impregnation/pyrolysis cycles, the samples were characterized to determine silicon distribution, mechanical properties, and oxidation properties.

Reviews of the theory and practice of supercritical fluid processing can be found in the literature<sup>3-5</sup>. Dense gases and liquids at conditions above their respective thermodynamic critical points are known as supercritical fluids. The supercritical regime is illustrated in Figure 2, a generalized phase diagram of a single component system. Table 1 lists the critical

## SUPERCRITICAL FLUIDS

- MANY GASES EXHIBIT ENHANCED SOLVENT POWER ABOVE THE CRITICAL POINT
- CRITICAL POINT FOR MANY GASES OF INTEREST ARE AT LOW TEMPERATURES AND MODERATE PRESSURES, E.G., CO<sub>2</sub>, 31°C, 73 ATM.
- GASES HAVE LOW VISCOSITY AND NO SURFACE TENSION, THEREFORE CAN PENETRATE FINE POROSITY
- SOLUTION ↔ PRECIPITATION CAN BE CONTROLLED BY CHANGES IN PRESSURE OR TEMPERATURE
- SCF IS ATTRACTIVE FOR BOTH EXTRACTION AND IMPREGNATION PROCESSES

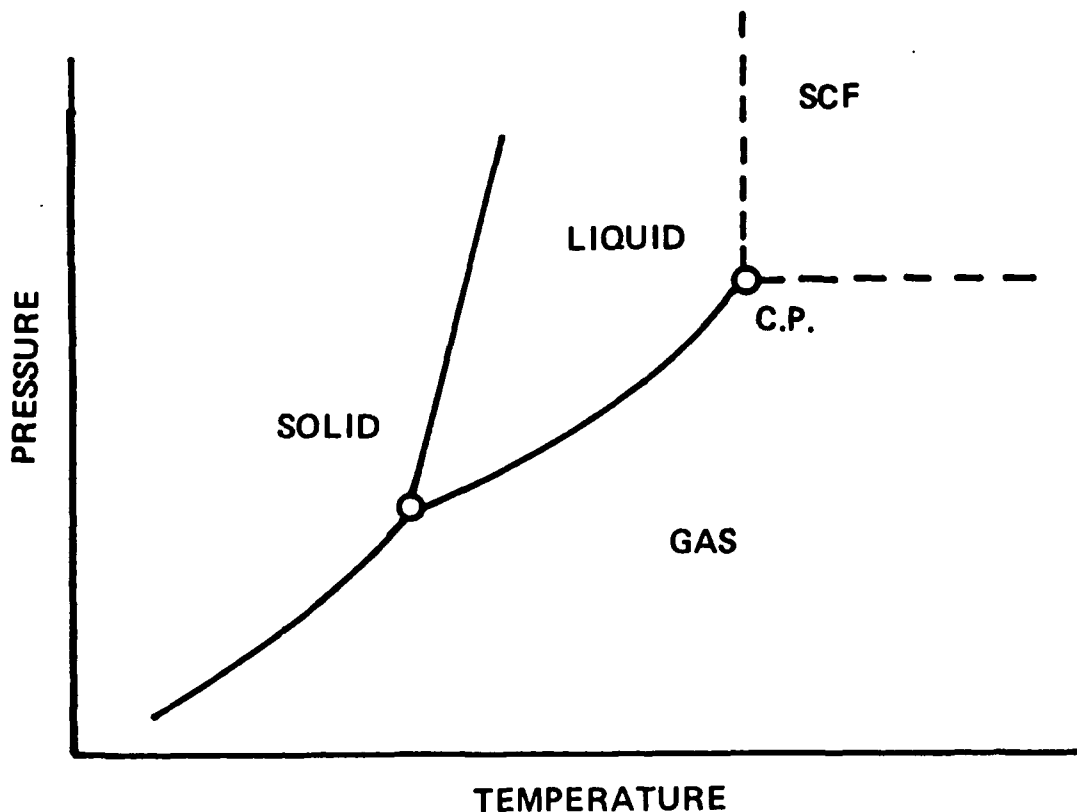


FIGURE 2 GENERALIZED P-T PHASE DIAGRAM FOR SINGLE COMPONENT SYSTEM SHOWING SUPERCRITICAL (SCF) REGIME

temperatures and pressures for a number of common gases which can be used as working fluids in supercritical fluid processing. The ability of high pressure gases to dissolve low vapor pressure materials was first reported by Hannay and Hogarth<sup>6</sup> in 1879. In 1955, Todd and Elgin<sup>7</sup> suggested that the pressure dependent dissolving power of supercritical fluids could be applied to chemical separation processes.

Table 1  
Critical Point Conditions  
for Common Gases

Fluid	T <sub>crit.</sub> (°C)	P <sub>crit.</sub> (atm)
Methane (CH <sub>4</sub> )	-82	46
Ethylene (C <sub>2</sub> H <sub>4</sub> )	10	50
Carbon dioxide (CO <sub>2</sub> )	31	73
Ethane (C <sub>2</sub> H <sub>6</sub> )	32	48
Nitrous oxide (N <sub>2</sub> O)	36.5	71
Propane (C <sub>3</sub> H <sub>8</sub> )	97	42

Supercritical fluid systems exhibit a number of unique properties which form the basis for their potential utility as processing tools:

- o Pressure-dependent solvent power
- o Near-ambient temperature processing capability
- o Useful mass transport properties of low viscosity and high diffusivity

- o Absence of surface tension

Table 2 compares the properties of supercritical fluids to gases and typical organic solvents. Supercritical fluids exhibit gas-like transport properties at densities approaching liquids.

Table 2  
Comparison of Properties of Supercritical Fluids and Organic Solvents

<u>Solvent</u>	<u>Diffusivity</u> cm <sup>2</sup> /sec	<u>Viscosity</u> cps	<u>Density</u> g/cc	<u>Surface Tension</u> dynes/cm
Gas	10 <sup>-1</sup>	10 <sup>-2</sup>	10 <sup>-3</sup>	0
Supercritical Fluid	10 <sup>-3</sup>	10 <sup>-1</sup>	0.6-1.0	0
Organic	10 <sup>-5</sup>	1	0.8-1.0	20-50

Under supercritical conditions, gases become exceptionally good solvents for materials which are normally considered insoluble in most solvents, i.e., materials with little or no vapor pressure. Furthermore, the solubility of dissolved materials is highly pressure dependent. Figure 3 illustrates the dramatic increase in solubility exhibited by two organic materials in supercritical ethylene and carbon dioxide, respectively. At low pressure, the solubility of the two materials is very low. However, after the pressure reaches some "threshold" level, solubility increases rapidly. This threshold pressure is near the critical pressure of the two fluids. The solubility calculated from vapor pressure considerations alone is shown at the bottom of Figure 3 as a cross for p - iodochlorobenzene at 100 atmospheres and as a circle for naphthalene at 200 atmospheres.



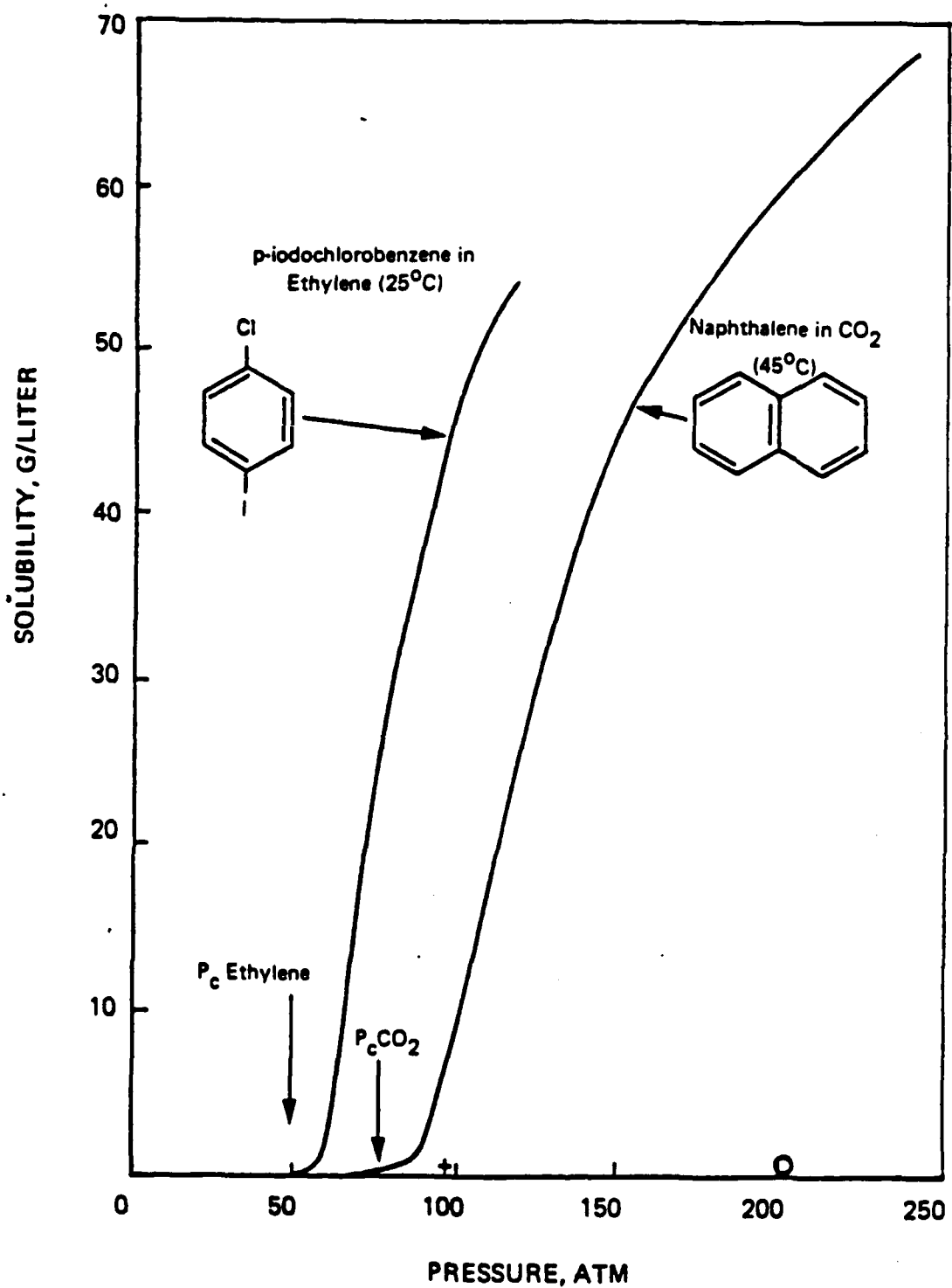


FIGURE 3 SOLUBILITY OF TWO ORGANIC COMPOUNDS IN SUPERCRITICAL FLUIDS

The solubility of any material in a supercritical fluid system can be expressed qualitatively in the form of a solubility map such as the solubility map for naphthalene in carbon dioxide shown in Figure 4. The features shown here are characteristic of all supercritical fluid systems. At sufficiently high pressures, the specific pressure level defined by the particular system, isobaric solubility increases as a function of temperature. At lower pressures, the solubility of a dissolved material is inversely related with temperature, a phenomenon not normally exhibited by solute/liquid solvent systems.

Supercritical fluids can be employed as pressure-dependent solvents for various organic extraction processes. A schematic diagram of such a process, is given in Figure 5. Four basic elements of the process are shown, viz., an extraction vessel, a pressure reduction valve, a separator for collecting the material dissolved in the extractor, and a compressor for recompressing and recycling fluid. (Ancillary pumps, valving, facilities for fluid make-up, heat exchangers for heating/cooling the fluid at various points in the process, and other similar equipment are omitted from the figure for clarity and ease of presentation). Useful quantitative aspects of the pressure and temperature dependence of solubility in a supercritical fluid system are detailed in Figure 4 which shows extensive data on the solubility of naphthalene in carbon dioxide. The solubility level of naphthalene can be changed by orders of magnitude with relatively small changes in temperature or pressure. Although solubility data for naphthalene in carbon dioxide will be used to explain the operation of a supercritical fluid process, the solubility behavior shown in Figure 4 is very general, applying to any material that dissolves to a modest extent in any supercritical fluid. The differences among various materials are only of degree, e.g., the solubility of some other material in some other fluid may be higher or lower than that of naphthalene, but the pressure-temperature-concentration curves will exhibit similar characteristics.

Reference to Figures 4 and 5 is made in explaining how a supercritical fluid extraction process operates. Some process operating parameters are indicated on two solubility isobars in Figure 4. Point 1

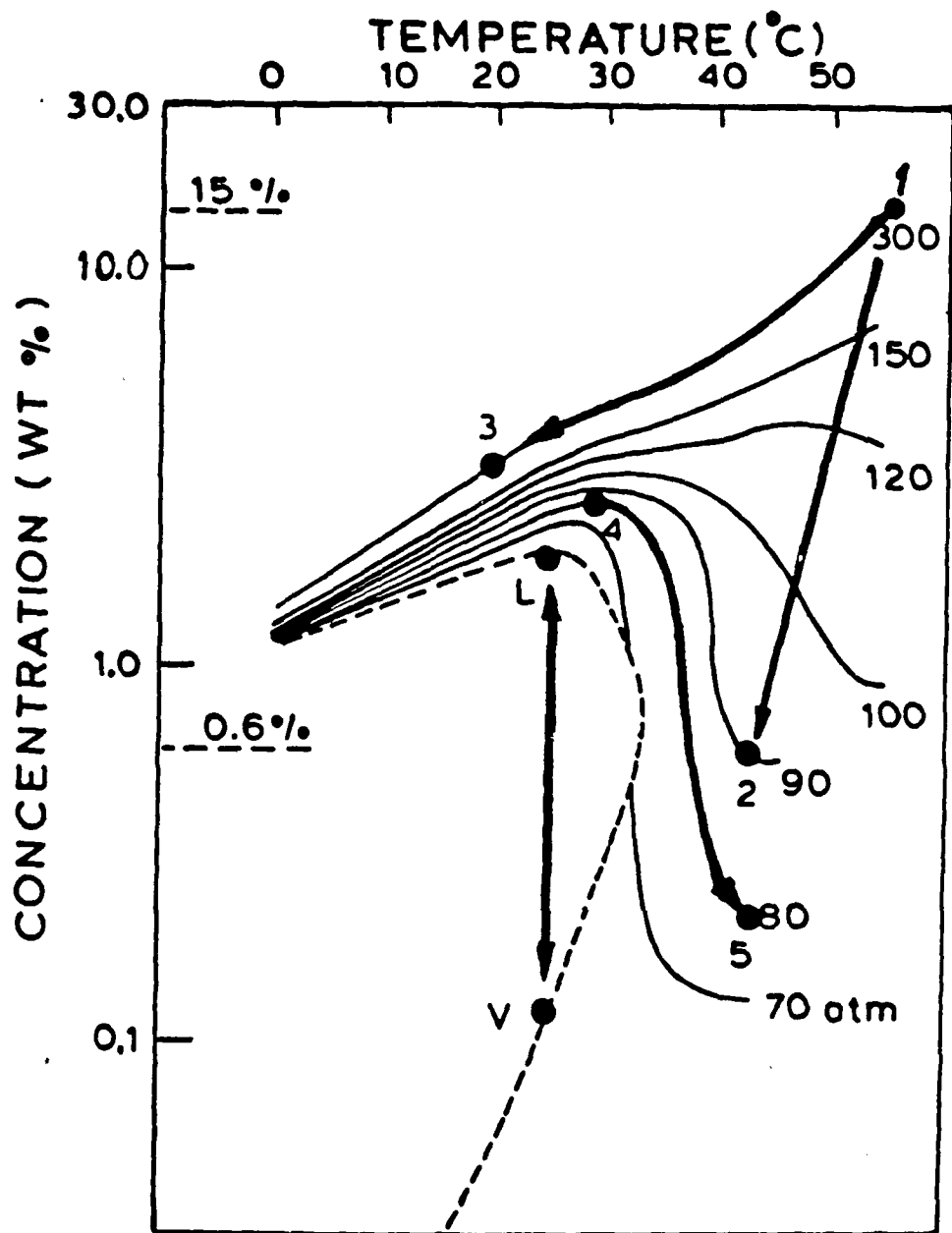


FIGURE 4 SOLUBILITY OF NAPHTHALENE IN CO<sub>2</sub>

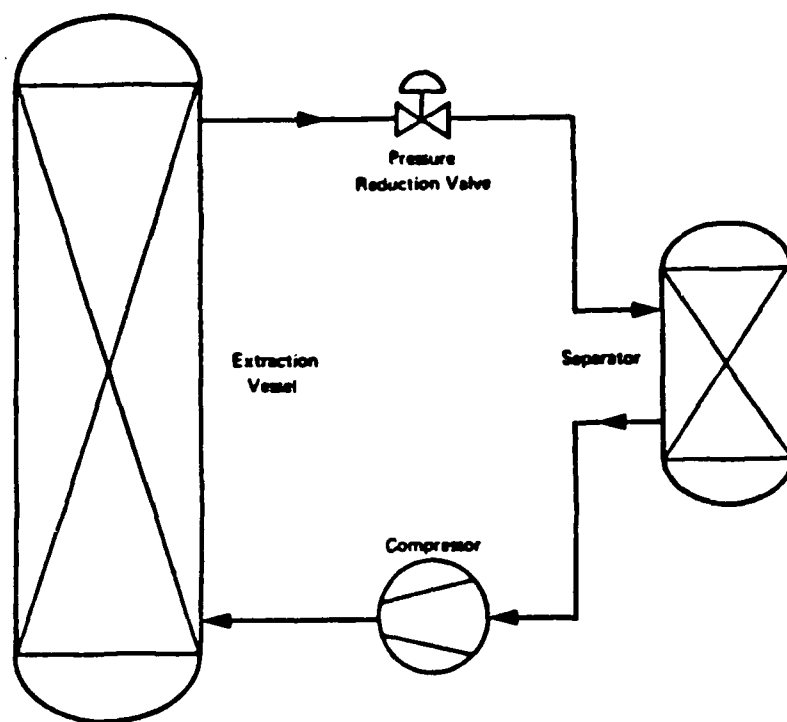


FIGURE 5 SCHEMATIC DIAGRAM OF A SUPERCRITICAL FLUID EXTRACTION PROCESS

represents conditions in the extractor, e.g., 300 atm, 43°C. The extractor vessel is assumed to be filled with naphthalene in admixture with another material which is insoluble in carbon dioxide and from which it is desired to remove the naphthalene. Supercritical carbon dioxide at condition 1 is passed through the extraction vessel wherein it dissolves (and extracts) the naphthalene from the insoluble material. The carbon dioxide-naphthalene solution leaving the extractor is expanded to 90 atm through the pressure reduction valve, as indicated by the directed path 1-2 in Figure 4. During the pressure reduction step, naphthalene precipitates from the solution, is collected in the separator, and the carbon dioxide leaving the separator is recompressed and returned to the extractor. This recycle process continues until all the naphthalene is dissolved and extracted, the directed line segment 1-2 in Figure 4 and its reverse on the solubility diagram representing approximately the cyclic process.

The applications discussed above utilize the dissolution/extraction properties of supercritical fluids to separate chemicals, seed oils, and the like. The inverse capability, i.e. the ability to deposit compounds from a supercritical fluid into a porous host material, has not been reported in the literature. The principal distinction between supercritical fluid extraction and impregnation is that the pressure/temperature change which results in solute precipitation occurs in the pressure vessel instead of across the pressure reduction valve. The porosity of the host sample then becomes the "collection vessel" for the precipitated solute. The unique transport properties and absence of surface tension of supercritical fluids greatly facilitate the penetration of microporous materials.

## 2.2 FIBER COATINGS

The mechanical properties of high temperature fiber reinforced composites is dependent upon the stability of the fiber/matrix interface and the formation of a controlled bond between the fiber and matrix. Fiber coatings may also be used to control the electrical or magnetic properties of a composite by the controlled application of conductive or insulating materials.

Fiber/matrix interface control is often accomplished by the application of non-reactive fiber coatings before or after preforming using CVD or sol-gel methods. However, processing temperatures and reactive gases such as chlorides and hydrogen required for CVD may cause fiber degradation rather than control it.

Surface tension considerations may prevent the application of sol-gel derived coatings on fiber preforms. Furthermore, sol-gel coatings may be limited to very thin coatings because of cracking due to drying shrinkage.

The unique transport properties of supercritical fluids and their pressure controlled deposition characteristics suggest that they may offer a useful alternative to other coating methods. Clearly, supercritical fluid coating is a special case of SCF impregnation in which the thickness is controlled by the initial polymer concentration. Other potential benefits include the near ambient processing conditions with non-reactive gases.

### 3.0 EXPERIMENTAL PROCEDURE

A process flow diagram is shown in Figure 6. Initial program effort was directed toward SCF polymer processing to establish the solubility conditions required to guide subsequent impregnation studies. Figure 7 details the polymer processing which includes both solubility measurements and polymer fractionation.

FIGURE 6

IMPREGNATION PROCESSING FLOW DIAGRAM

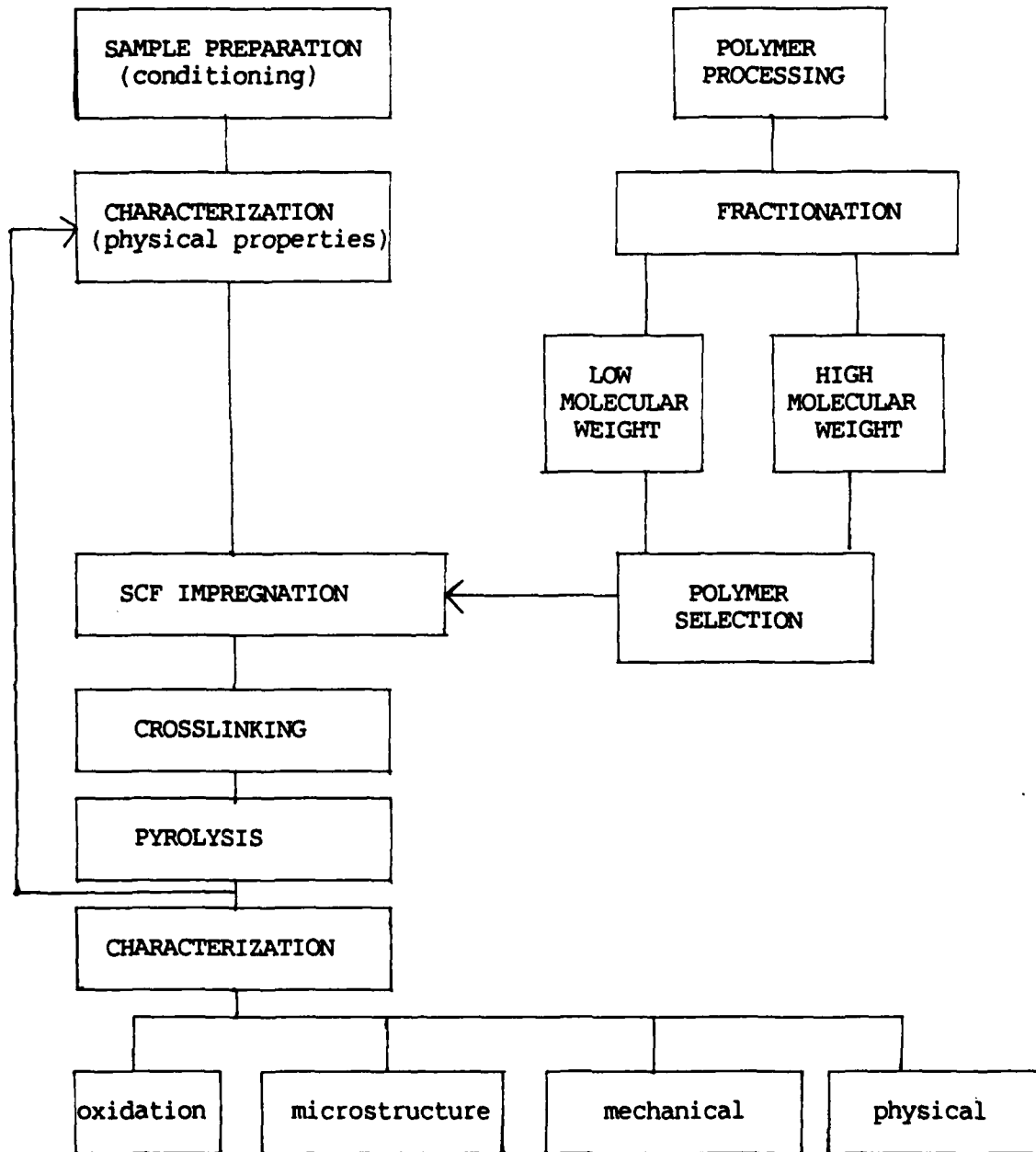
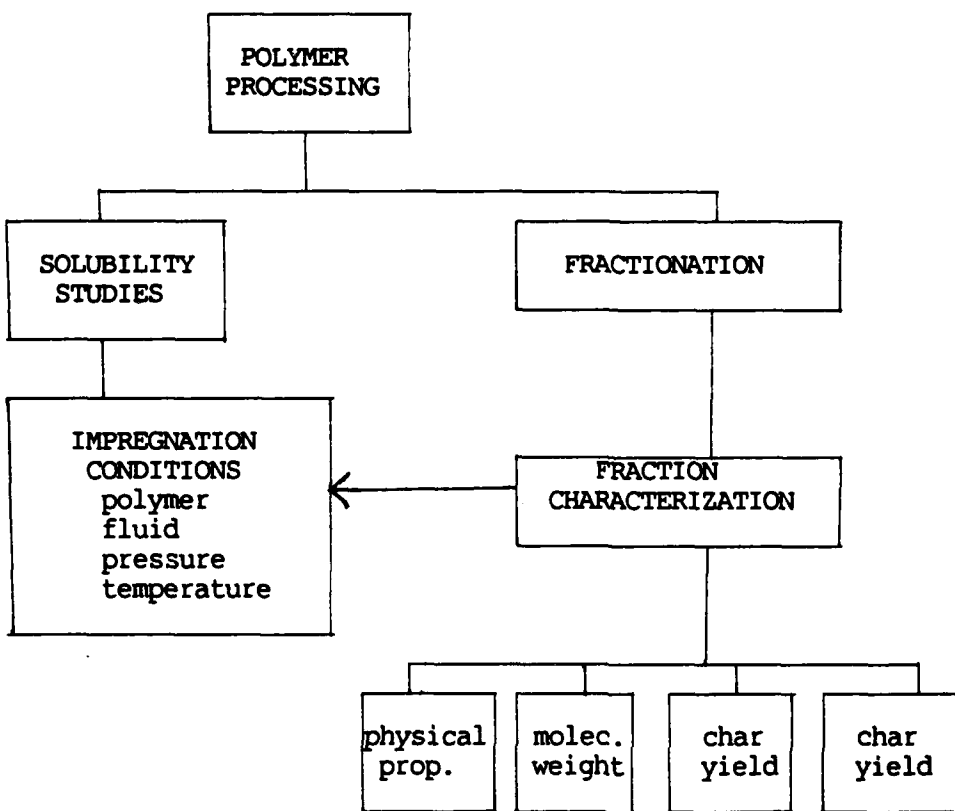


FIGURE 7  
POLYMER PROCESSING FLOW DIAGRAM





### 3.1 Polymeric Precursors

Commercially available precursors to carbon and silicon carbide obtained for solubility and impregnation studies are given in Table 3. Yajima<sup>3</sup> and Schilling<sup>4</sup> described the synthesis and properties of polycarbosilane and vinylic polysilane respectively. As shown in the table, polycarbosilane is a solid and the vinylic polysilane is a liquid polymer. Polycarbosilane was used for most of the program because it was readily available and would serve as a model system to demonstrate the feasibility of using supercritical fluids to impregnate porous hosts with an oxidation resistant material. Recent developments in oxidation resistant carbon/carbon suggesting other chemistries which would form low melting point glasses and effectively seal pores provide the basis for future work in this area.

The concept of "volume yield" must be considered for any process involving precursor materials. Volumetric yield is defined as the ratio of char volume to precursor volume and combines the effects of pyrolysis weight loss and the increased density of the char. For the silicon carbide precursors used in this study, the volumetric yield is about 30 percent. Assuming complete pore filling, the new porosity following each impregnation and pyrolysis cycle should be 70 percent of the last porosity value. Therefore two impregnation/pyrolysis cycles would be required to decrease the starting porosity by one half.

TABLE 3  
CARBON AND SILICON CARBIDE PRECURSORS

<u>PRODUCT</u>	<u>TYPE</u>	<u>SUPPLIER</u>	<u>PHYSICAL FORM</u>
15 Vacuum	Coal Tar Pitch	Allied Chemical	Solid
Furcarb	Furfural Phenolic Resin	QO Chemicals	Liquid
FA	Furfural Alcohol	QO Chemicals	Liquid
SC1008	Phenolic Resin	Borden Chemical	Liquid
X9-6348	Polycarbosilane	Nippon Carbon	Solid
*	Vinylic Polysilane	Union Carbide	Liquid

### 3.2 Porous Host Samples

Preliminary testing was conducted using a discontinuous fiber insulation material, CARBOND, obtained from Carbon Technologies. This material consists of short carbon fibers bonded at fiber contact points by phenolic resin and exhibits 85 to 90 percent apparent porosity. The high porosity was expected to result in large impregnation weight gains and thus be more sensitive to process variations. Additionally, the absence of metallic impurities simplified the identification of polymer deposits.

HITCO ACC4, ACC2, ACCO (T300 fibers, high temperature stabilized, 8 harness satin weave, warp aligned, phenolic resin matrix) were selected as the carbon/carbon host samples. Using these materials, the effectiveness of the SCF process could be determined over a porosity range of 6 to 23 percent.

Because the mechanical properties of inhibited 2D substrates are considered only barely adequate, there will be growing interest in the

development of inhibition systems for 3D material. Particulate loaded prepreg based inhibition systems cannot be readily adapted to the 3D architecture. In recognition of this, pore coating was identified as an area where more development was needed.

Samples of 3D carbon/carbon were obtained from F.A. Iannuzzi of Southern Research Institute. The 3D AVCO 223 material was selected primarily because of its low apparent porosity (about four percent) and dense microstructure.

All carbon/carbon samples were initially conditioned by heating in argon to the desired pyrolysis temperature (either 1000°C or 1400°C). This was done to stabilize the microstructure and avoid polymer char disruption by continued volatilization of the resin matrix.

Following the initial conditioning, samples were characterized in terms of initial weight, bulk density, and apparent porosity.

### 3.3 Laboratory Procedure for Deposition of Ceramic Precursors

A schematic diagram of the equipment installed at PHASEX and B&W is shown in Figure 8. The system is composed of a bank of gas cylinders for supplying gas to a high pressure diaphragm-compressor, a vessel downstream of the compressor which is filled with a material to be dissolved (and when impregnation studies are carried out, also with the body to be impregnated), associated pressure and temperature control devices (not shown in the diagram), and a pressure reduction valve to control the flow rate through the compounds (or the host body). If a solubility value is to be determined, an amount of material is precipitated downstream of the pressure reduction valve, collected, and weighed, and its concentration in the supercritical fluid solution is calculated from the integrated gas volume measured by a dry test meter.

A Newport Scientific supercritical fluid extraction system was purchased and modified to permit remote operation at B&W. The pressure vessel was located in a bunker and controlled from a console outside the

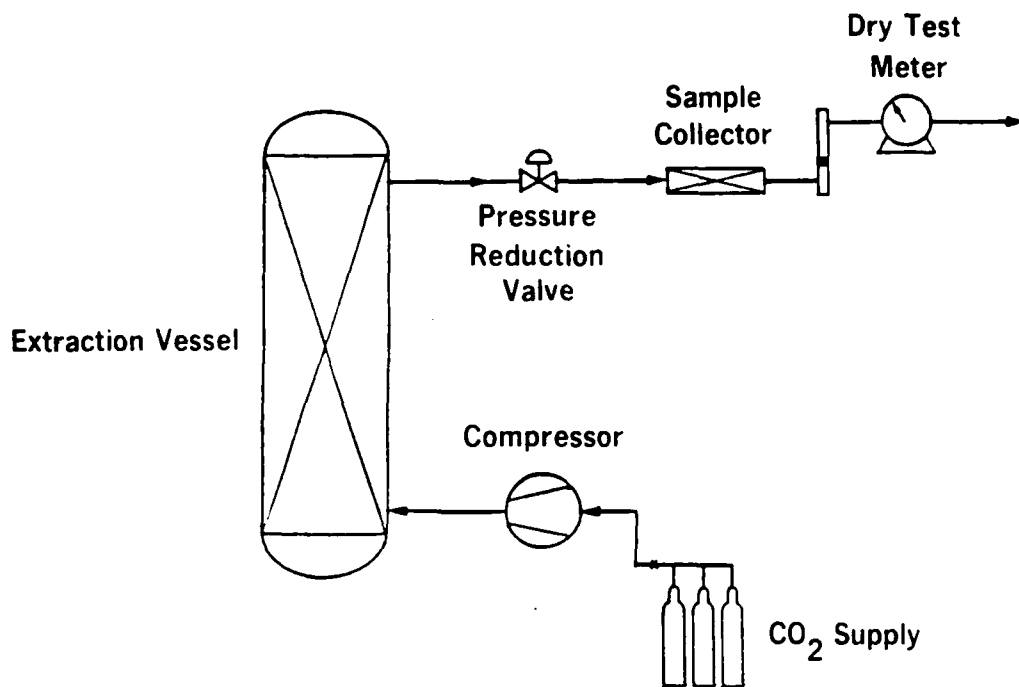


FIGURE 8 EXPERIMENTAL APPARATUS FOR SUPERCRITICAL FLUID EXTRACTION AND IMPREGNATION

bunker. Additional safety features include a combustible gas detector and associated solenoid valves which isolate the pressure vessel and propane supply either manually or due to combustible gas alarm. A key component of the remote operation is the air operated pressure reduction valve which allows controlled system venting from the console. Vented propane is diluted below the explosive concentration and exhausted through a stack.

Process temperature and pressure are controlled from the console and recorded on a dual pen strip chart recorder. Temperature is monitored by a type J thermocouple located inside the vessel at the sample position. A Dynisco pressure transducer provides a zero to five volt output which corresponds to zero to 10,000 psi as the pressure signal.

An example of the process data from a typical impregnation run is shown in Figure 9. Following an initial carbon dioxide purge, the vessel was isolated and heated to above the propane critical temperature. At this point, the vessel was purged with propane and pressurized in a stepwise manner to 7000 psi as heating continued to 180°C. After the desired hold, the heater was turned off and the vessel allowed to cool. The availability of detailed process data will be used to guide future process optimization studies.

#### 3.4 POLYMER SOLUBILITY MEASUREMENTS

Several polymers were very quickly screened for their solubility characteristics. A schematic diagram of the apparatus used is shown in Figure 8. Solubility measurements consisted of flowing supercritical fluid through the vessel containing the polymer. As the supercritical fluid passes through the vessel, it dissolves the polymer; the solubility is a function of many factors, e.g., the gas used (i.e., whether it is carbon dioxide or propane, for example) the pressure, temperature, polymer, and the molecular weight distribution of the polymer. The solution of the polymer and the supercritical fluid leaving the vessel is expanded to one atmosphere and the dissolved polymer nucleates and precipitates from the gas phase and is collected in a standard 200 mm drying (U) tube. The mass of the collected material along with the volume

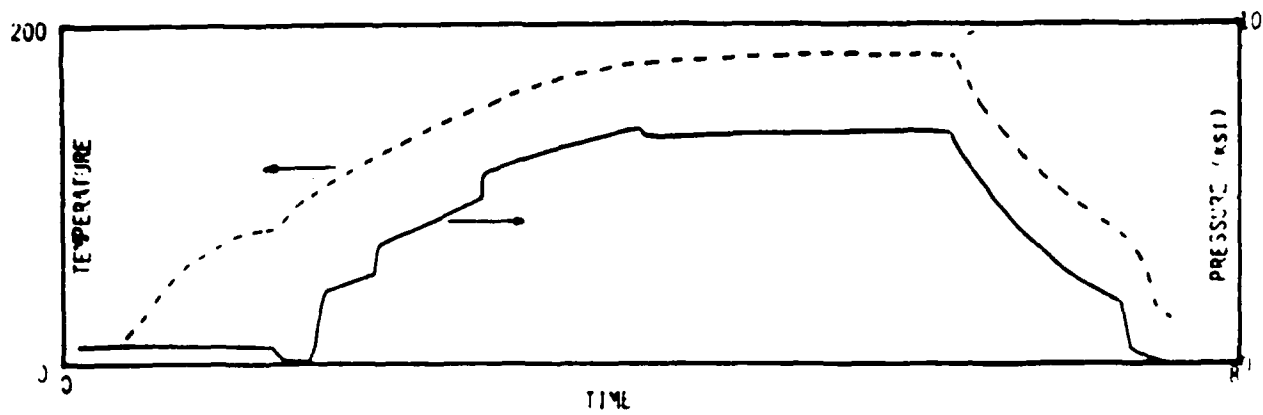


FIGURE 9 IMPREGNATION CYCLE PROCESS DATA

of gas used to extract this material allows a solubility level to be determined.

Solubility determinations were conducted by sequential extractions as described above of material from an initial sample charge at successively increasing pressures and temperatures. In addition, other gases were sometimes included to check its solvent power at one condition of elevated temperature and pressure after completing a test series with the initial test solvent gas.

To gain a better understanding of the solution/precipitation process, Dr. Mark McHugh, Johns Hopkins University, conducted polycarbosilane (PCS) tests in a variable volume SCF view cell shown in schematic form in Figure 10. By varying cell volume, solubility conditions of temperature and pressure can be varied up to 150°C and 6000 psig respectively at constant composition. A boroscope attached to a video camera and recorder provided a permanent record of experimental details and allowed repeated review of rapidly changing events.

### 3.5 Polymer Fractionation

Selected polymers were fractionated using sequential extractions at increasing pressures and temperatures. At each pressure/temperature condition, the supercritical fluid was allowed to flow over the polymer until no further precipitation occurred in the collection vessel. Fractionation differs from solubility measurements by intentionally depleting the polymer sample before proceeding to the next test condition.

The molecular weight distribution in each fraction is inversely related to the number of fractions. Improved molecular weight control can be achieved by using a fluid which exhibits low to moderate solubility for the test polymer.

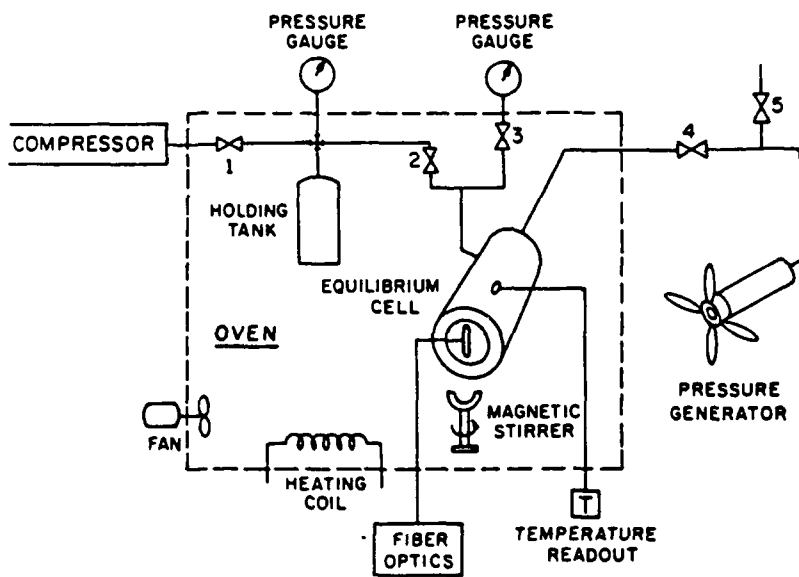


FIGURE 10  
 Schematic Diagram of Constant Composition View Cell  
 (Krukonis and McHugh 1986)



## 4.0 RESULTS AND DISCUSSION

### 4.1 Solubility Results

The polymers which were tested for solubility in supercritical fluids included SC-1008, a phenolic resin; 15 vacuum pitch, a coal tar pitch; and Furcarb, a furfuryl alcohol polymer. In the preliminary series, supercritical carbon dioxide and propane were tested in a scoping evaluation. It was found that the respective polymers were not dissolved completely in carbon dioxide or in propane at conditions of temperature and pressure up to 200°C and 7000 psi. It was found, furthermore, that the respective polymers are composed of a wide molecular weight range of oligomers as the descriptions in Tables 4, 5, and 6 show.

For example, and referring to Table 4, the SC1008 phenolic resin tested is an orange brown medium viscosity liquid. For comparative purposes at room temperature it pours like room temperature maple syrup. Note that extract #1 is described as a water white low viscosity liquid (probably the isopropanol carrier solvent) pointing out that low molecular weights are extracted at the conditions shown. Table 5 gives similar descriptions for the Furcarb furfural phenolic resin and respective fractions.

The 15 vacuum coal tar pitch described in Table 6 resulted in extraction fractions which are colored quite differently from the parent material. Color, viscosity, and melting point differences (or melting range) are frequently satisfactory as rather simple techniques for determining qualitatively the distribution of molecular weights of a parent material. In a polymer which is known to be composed of homologous series members, viscosity is especially quantitative as a tool for determining molecular weight distribution.

The solubility of polycarbosilane in propane was measured at 120°C as a function of pressure. The results shown in Figure 11 are similar to the naphthalene results discussed previously and are the key to both the impregnation of porous hosts with supercritical solutions and

# Solubility of Polycarbosilane

Lot 308052

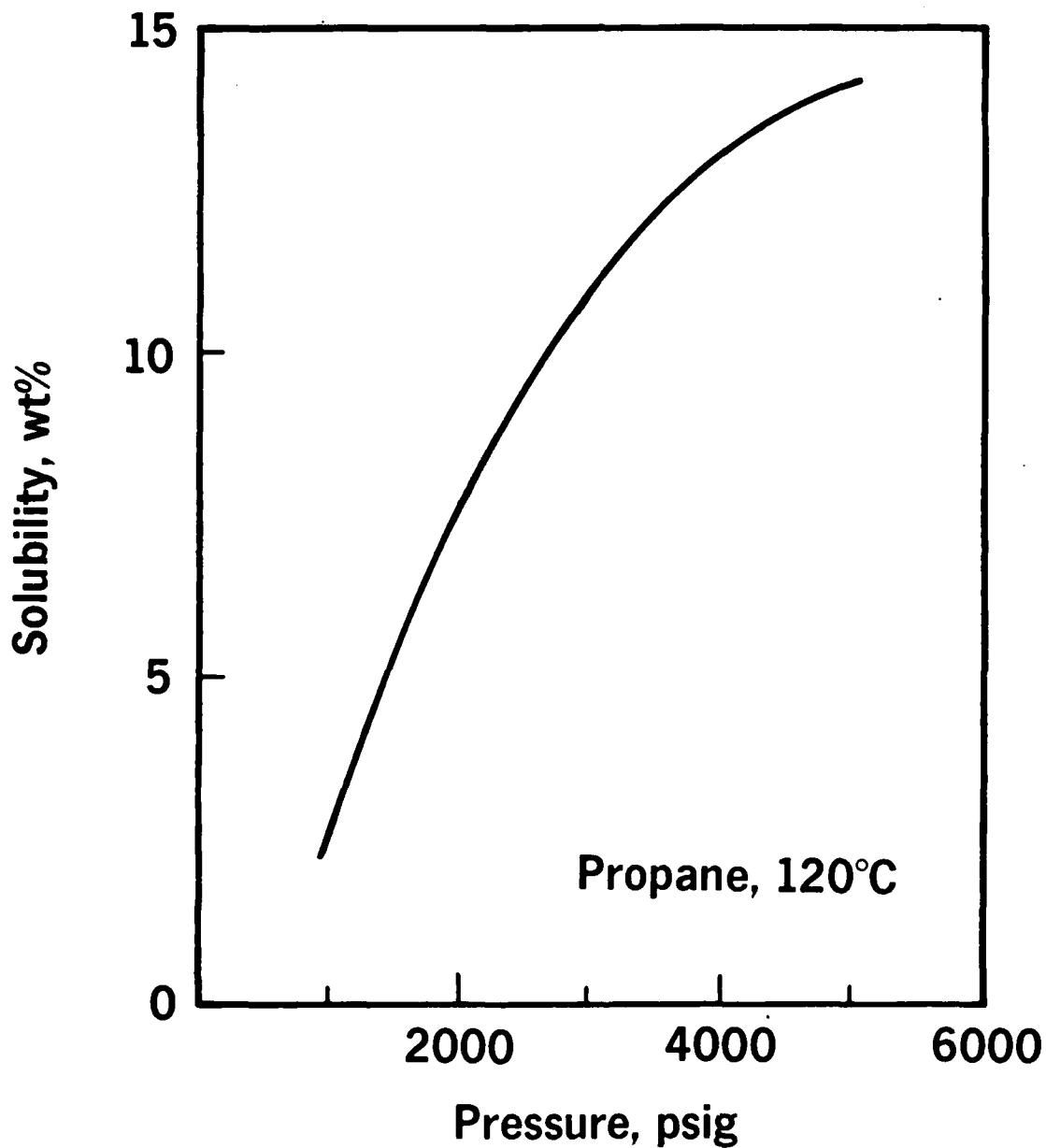


FIGURE 11 SOLUBILITY OF POLYCARBOSILANE

polymer fractionation. Note that polycarbosilane and polysilane are completely soluble in supercritical propane leaving no undissolved residue in the extraction vessel.

TABLE 4  
SOLUBILITY RESULTS FOR SC1008 (PHENOLIC RESIN)

<u>FRACTION</u>	<u>GAS</u>	<u>PRESSURE</u> <u>(PSI)</u>	<u>TEMP.</u> <u>(°C)</u>	<u>GAS</u> <u>QUANTITY</u>	<u>EXTRACTED</u> <u>WEIGHT</u>	<u>OBSERVATIONS</u>
28-1	CO <sub>2</sub>	3000	90	300 G	2.72 G	Water White Liquid
28-2	CO <sub>2</sub>	3000	90	800 G	0.35 G	White, Opaque Semi-Solid
28-3	Propane	5000	110	400 G	<0.02	N.A.

INITIAL CHARGE WEIGHT = 8.38 G  
CHARACTERISTICS: MEDIUM VISCOSITY, ORANGE BROWN LIQUID  
TOTAL WEIGHT COLLECTED = 3.07 G (36.6%)  
RESIDUAL MATERIALS ON FILTERS WAS SOLID

TABLE 5  
SOLUBILITY RESULTS FOR FURCARB (FURFURAL PHENOLIC RESIN)

<u>FRACTION</u>	<u>GAS</u>	<u>PRESSURE</u> <u>(PSI)</u>	<u>TEMP</u> <u>(C°)</u>	<u>GAS</u> <u>QUANTITY</u>	<u>EXTRACTED</u> <u>WEIGHT</u>	<u>OBSERVATIONS</u>
29-1	CO <sub>2</sub>	5800	90	800	3.16	Water White Liquid
29-1	Propane	5500	110	200	0.17	Brown, Semi-Solid

INITIAL CHARGE WEIGHT = 10.82 G  
CHARACTERISTICS - LOW VISCOSITY, ORANGE LIQUID  
TOTAL WEIGHT COLLECTED = 3.33 (30.8%)  
RESIDUAL MATERIAL ON FILTERS WAS SOLID.

TABLE 6  
SOLUBILITY RESULTS FOR 15 VACUUM COAL TAR PITCH

<u>FRACTION</u>	<u>GAS</u>	<u>PRESSURE</u> (PSI)	<u>TEMP</u> (°C)	<u>GAS</u> <u>QUANTITY</u> (G)	<u>EXTRACTED</u> <u>WEIGHT</u> (G)	<u>OBSERVATIONS</u>
30-1	Propane	2000	120	200	0.76	Orange, Semi-Solid
30-2	Propane	3300	120	400	1.92	Brown, Semi-Solid
30-3	Propane	3300	200	500	1.42	Dark Brown, Semi-solid
30-4	Propane	7000	200	200	0.82	Dark Brown, Solid

INITIAL CHARGE WEIGHT = 11.12 G

CHARACTERISTICS: BLACK, FRIABLE SOLID

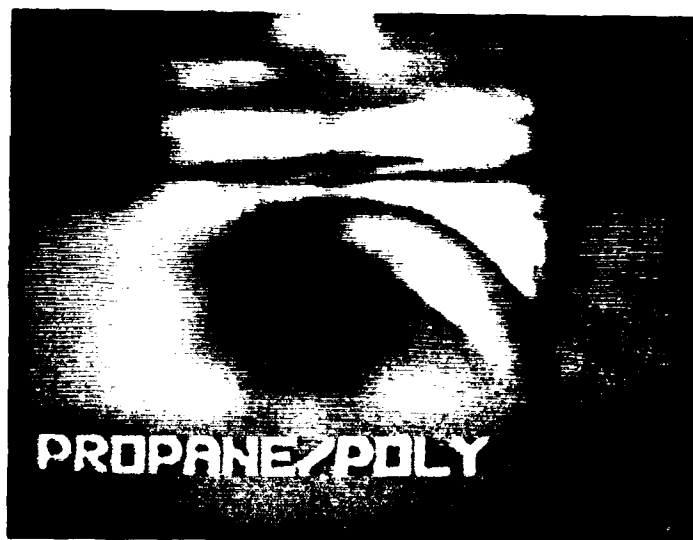
TOTAL WEIGHT COLLECTED 4.92 G (44.2%)

RESIDUAL MATERIAL ON FILTERS WAS SOLID AND POWDERED.

The initial view cell experiment consisted of a 0.7 gram piece of parent polymer in 12 grams of propane as shown in Figures 12A and B. Note that this composition remained constant during the entire experiment because pressure was controlled by a movable piston and not by pumping in additional



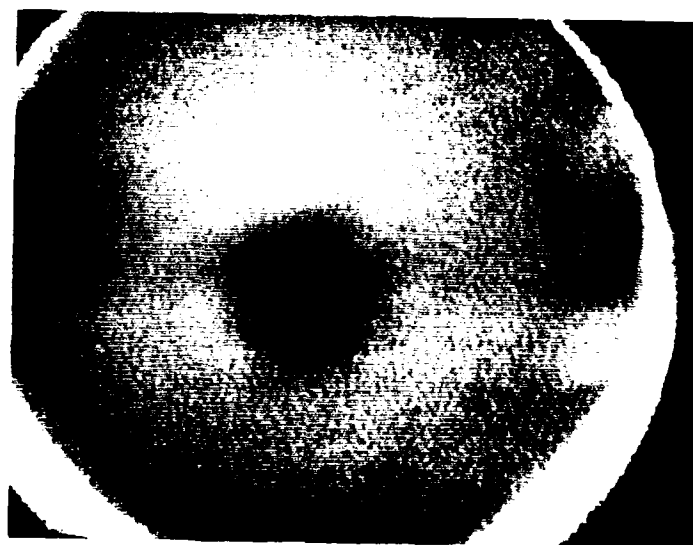
A



B



C



D

FIGURE 12 VIEW CELL SOLUBILITY/PRECIPITATION SEQUENCE

propane which decreases the polymer concentration. Figure 12A shows the polycarbosilane piece in the lower left corner of the photo with the out of focus image of the stirring bar in the back of the vessel. The liquid propane level is apparent just above the stirring bar in Figure 12B.

Figures 12B and C show a pressure drop sequence at 115°C from 5500 psig in Figure 12B to cloud point in Figure 12C at 4900 psig. The bright background in each photograph is the movable piston which is controlled by a hand operated pump. A glass encased magnetic stirring bar is located in front of the piston. The smaller dark spot in the center of each photograph was an artifact of the optical system.

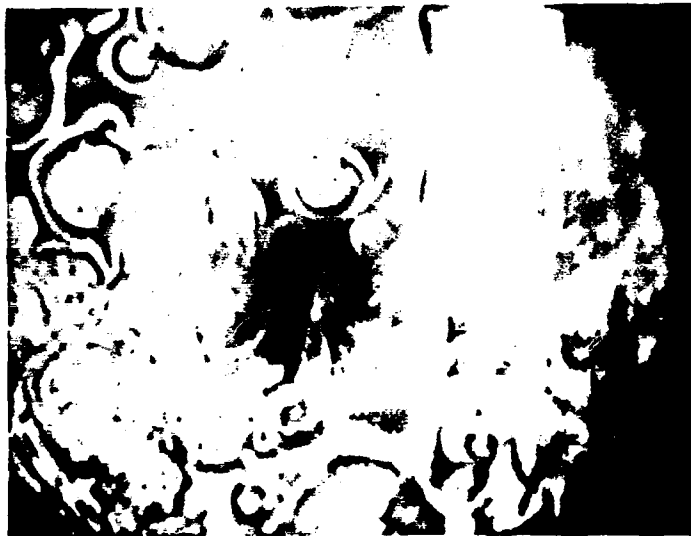
Because of the broad molecular weight distribution of PCS and its relatively low melting point, a cloud point is observed as opposed to a solid particle "snow" sometimes observed with compounds such as naphthalene. Future work may require the use of narrow molecular weight fractions to better define phase boundaries. Perhaps a minus 1000 psi fraction and plus 6000 psi fraction would establish the boundaries of the parent polymer and guide future processing developments.

Although the cell appeared clear when the pressure was increased back to 5000 psig at 108°C, the magnetic stirring bar was coated with a viscous liquid second phase. This material was most likely the highest molecular weight fractions of the parent polymer which remained undissolved at these conditions of temperature and pressure. Figure 13A shows the inside surface of the sight glass where the stirring bar contacted and left a smear of the viscous high molecular weight polymer fractions. In an attempt to dissolve the smear by increasing pressure, the rupture disc failed and the fully precipitated condition shown in Figure 13B resulted.

The appearance of the stirring bar and sight glass coatings demonstrated the importance of assuring complete solubility during an impregnation run to avoid surface sealing and the resultant decrease in permeability to the sample interior. Tendencies to form viscous second phases will need to be considered in the selection of polymers or polymer fractions and process conditions in future work. In addition, it may be necessary to



A



B

FIGURE 13 VIEW CELL DEPOSIT AND RAPID PRECIPITATION  
RESULT

limit polymer concentration to ensure complete solubility at impregnation conditions of temperature and pressure in order to minimize host coating and maximize penetration/deposition.

#### 4.2 SCF FRACTIONATION RESULTS

PCS and polysilane were fractionated at pressures up to 6500 psi and temperatures up to 170°C. Molecular weights of parent PCS material and individual fractions were determined by gel permeation chromatography (GPC), and the results are given in Figure 14 as molecular weight distributions. Two lots of PCS polymer were separated into six and eight fractions, respectively; however, only high, medium, and low molecular weight cuts are shown for clarity. It is apparent from the figure that the increased number of fractions in lot 403079 resulted in narrower cuts in terms of molecular weight distribution.

Polysilane was fractionated using carbon dioxide and propane at increasing pressures and temperatures to develop solubility behavior and char yield trends. Results of this fractionation are shown in Table 7.



# GPC Results for Two Lots of Polycarbosilane

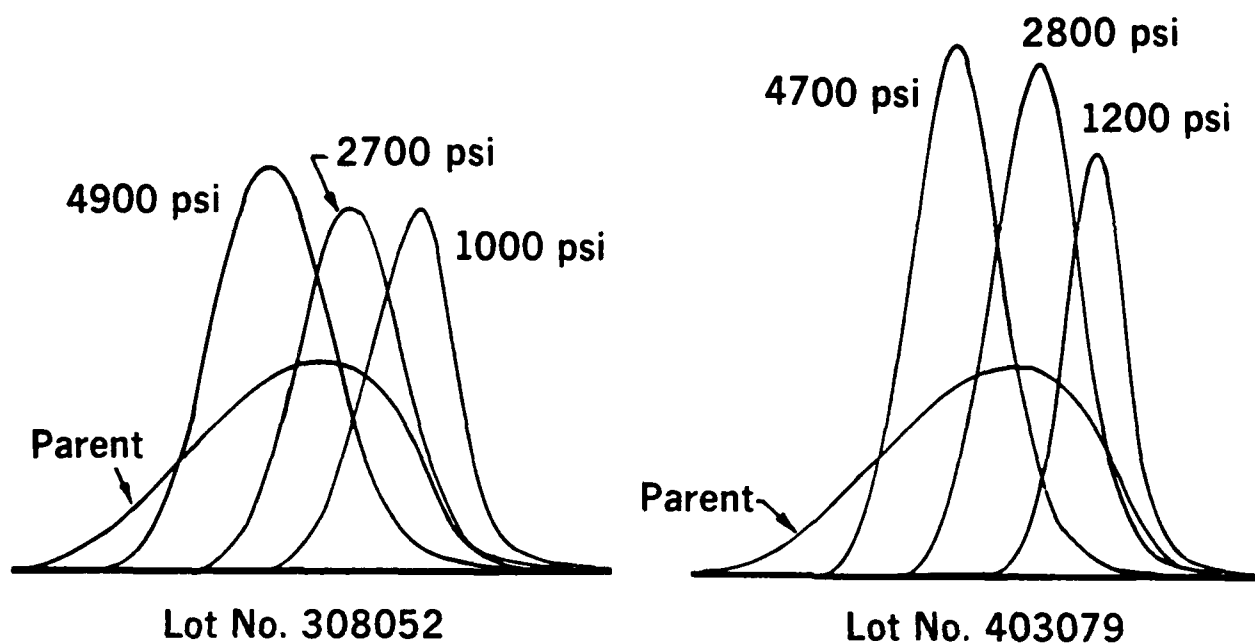


FIGURE 14 GPC RESULTS FOR TWO LOTS OF POLYCARBOSILANE

Table 7 UC Polysilane Fractionation Results

Sample	Fluid	Pressure (psi)	Temp. (°C)	Extracted Percent	Description
282-1	CO <sub>2</sub>	3000	65	14.0	clear liquid
282-2	CO <sub>2</sub>	5500	100	20.8	clear liquid
282-3	CO <sub>2</sub>	5500	100	11.6	clear coating
282-4	propane	1400	100	21.3	sticky foam
282-5	propane	5000	110	19.2	solid foam
282-6	propane	6000	110	N.D.	porous particles

The wide range of physical properties exhibited by SCF derived fractions allows a significant measure of process control not readily available by other means. Ability to control both viscosity and molecular weight distribution may result in improved control of such processes as fiberization and cloth prepregging operations.

#### 4.3 Pyrolysis Results

Polycarbosilane and polysilane fractions were pyrolyzed in fused quartz crucibles to 1000°C in argon at a heating rate of 1°C per minute. Char yield results for polycarbosilane and polysilane are given in Figures 15 and 16 respectively. Note that the low molecular weight fractions of both polymers exhibit very low yields. Because initial impregnations with parent polycarbosilane often resulted in low insitu char yield, it was assumed that a

# Polycarbosilane 1000C Char Yield

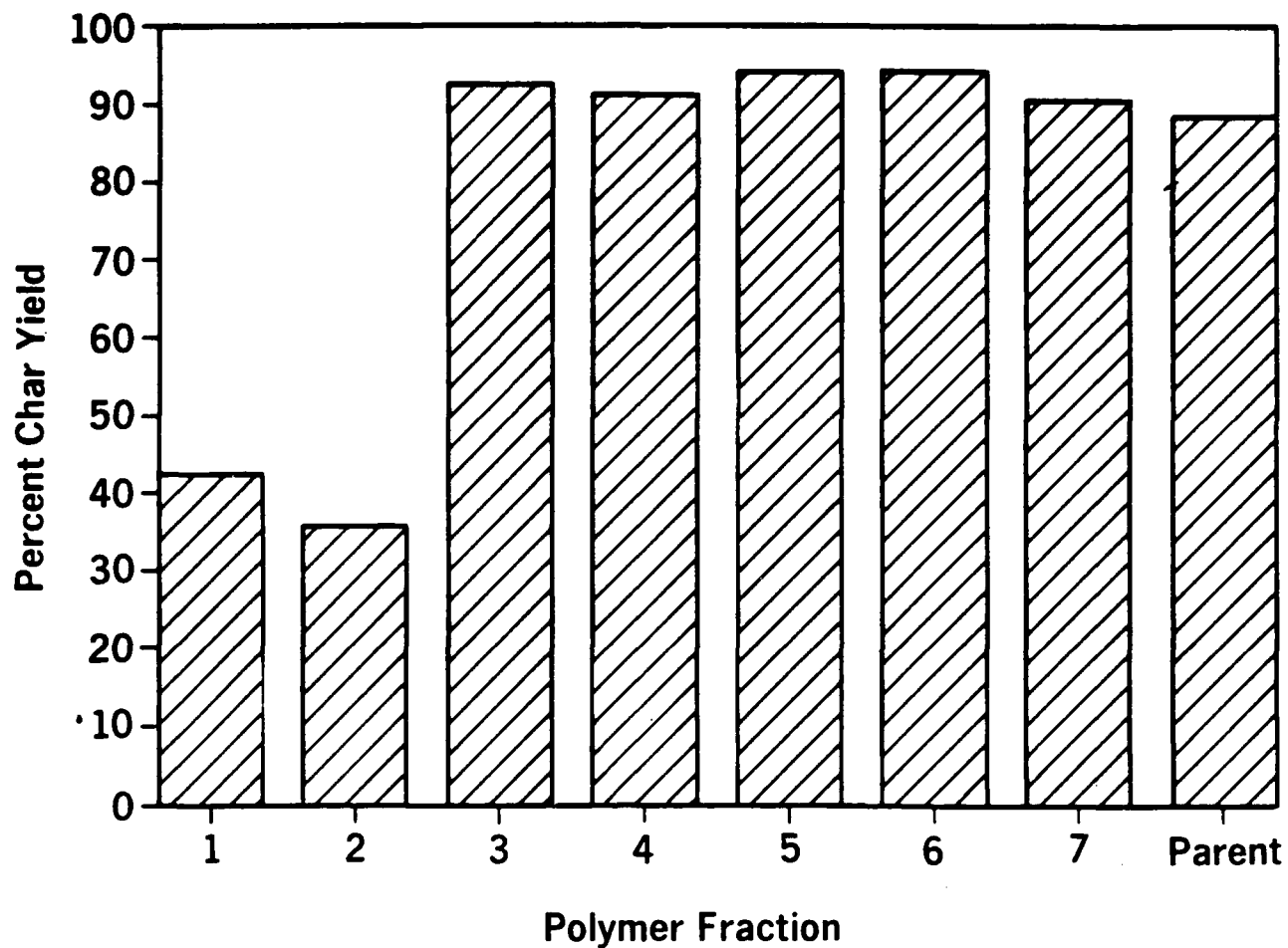


FIGURE 15 POLYCARBOSILANE 1000°C CHAR YIELD

# UCPS 1000 C Char Yield

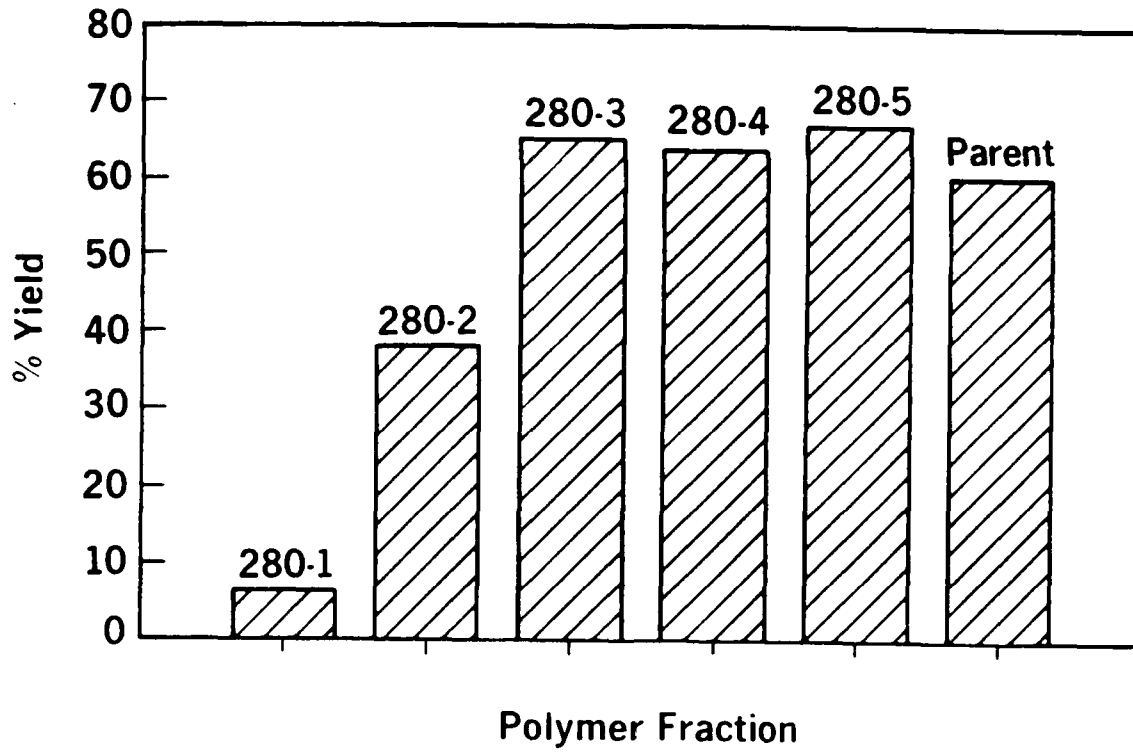


FIGURE 16 UCPS 1000°C CHAR YIELD

disproportionate amount of low molecular weight had been dissolved and deposited in the host sample. Subsequent runs avoided this problem by SCF refinement of parent polymer to eliminate low char yield fractions.

#### 4.4 IMPREGNATION RESULTS

Impregnation effectiveness was monitored by measuring weight gain, bulk density, and apparent porosity after each process cycle. Typical results are shown in Figures (17, 18, and 19) for polycarbosilane impregnated ACC2.

The weight change data shown in Figure 17, are grouped into two sets which are related to the SCF precipitation method employed. The two upper curves represent samples which were impregnated using a temperature drop precipitation. Slightly less efficient impregnation resulted from a pressure drop precipitation at constant temperature as indicated by the lower curves.

Sample bulk densities increased from 1.63 g/cc to about 1.72 g/cc, Figure 18, as the apparent porosity decreased by one half after six impregnations, Figure 19.

In situ char yields determined after each impregnation/pyrolysis cycle varied from 50 to 70 percent for the high molecular weight polymer fraction used in this series. Sample pyrolysis was accomplished by heating to 1000°C in argon at 1°C per minute with a four hour hold at maximum temperature.

The SCF impregnation process must be considered as one component of a total oxidation protection system. To evaluate the contribution of the SCF impregnation, twenty ACC4 samples were obtained from J. Strife at United Technology Research Center (UTRC). After six SCF impregnations with polycarbosilane, the samples exhibited a 4.01 percent weight gain, a bulk density increase from 1.65 g/cc to 1.72 g/cc, and an apparent porosity decrease from 9.90 percent to 7.24 percent. The samples were returned to UTRC to receive the balance of the oxidation protection system which is based on a CVD silicon nitride coating. UTRC will then compare these samples to standard samples using a MCAIR oxidation test cycle.

# Percent Weight Gain

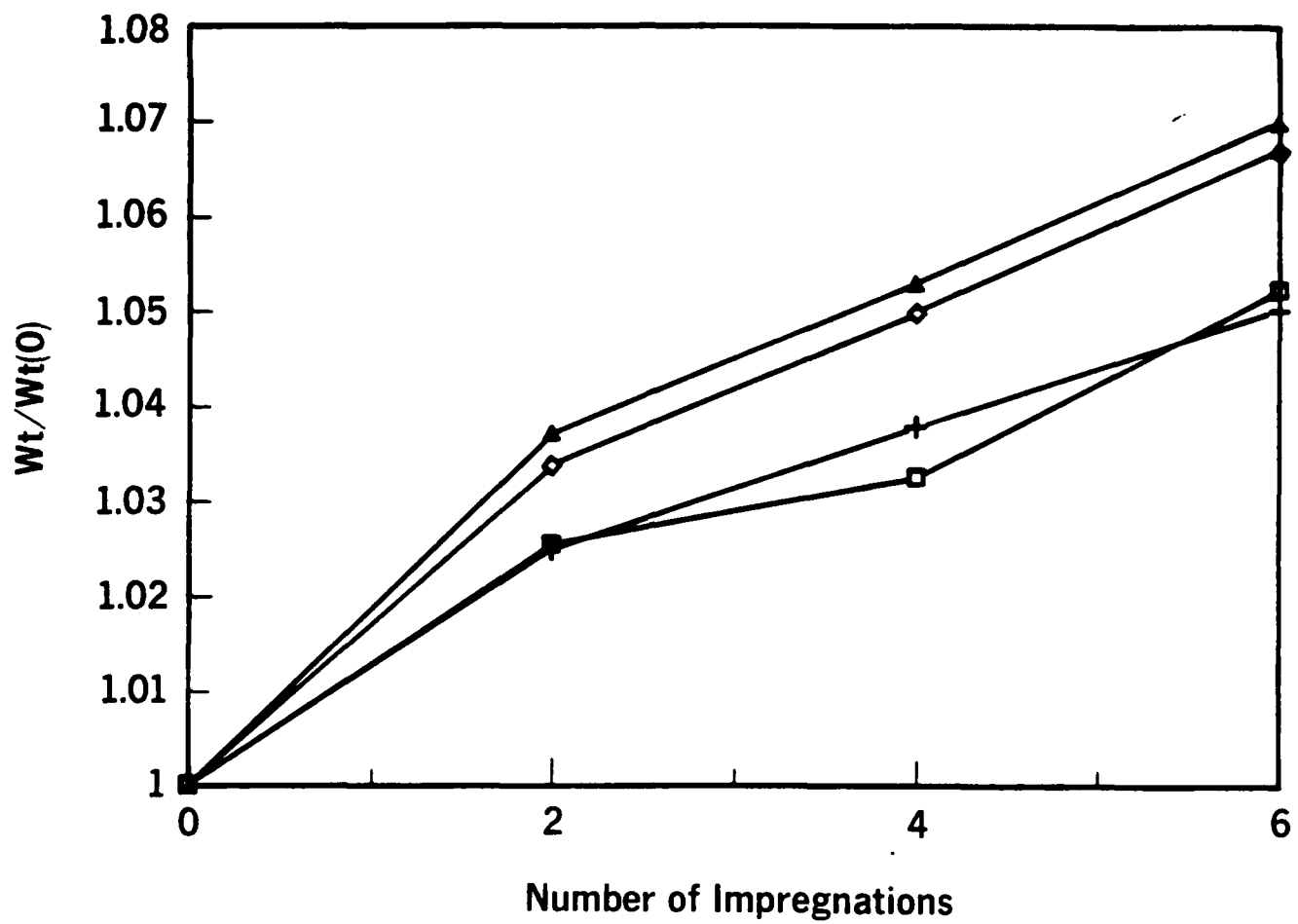


FIGURE 17 ACC2 IMPREGNATION WEIGHT GAIN

# Density Change

ACC2 (1000C)

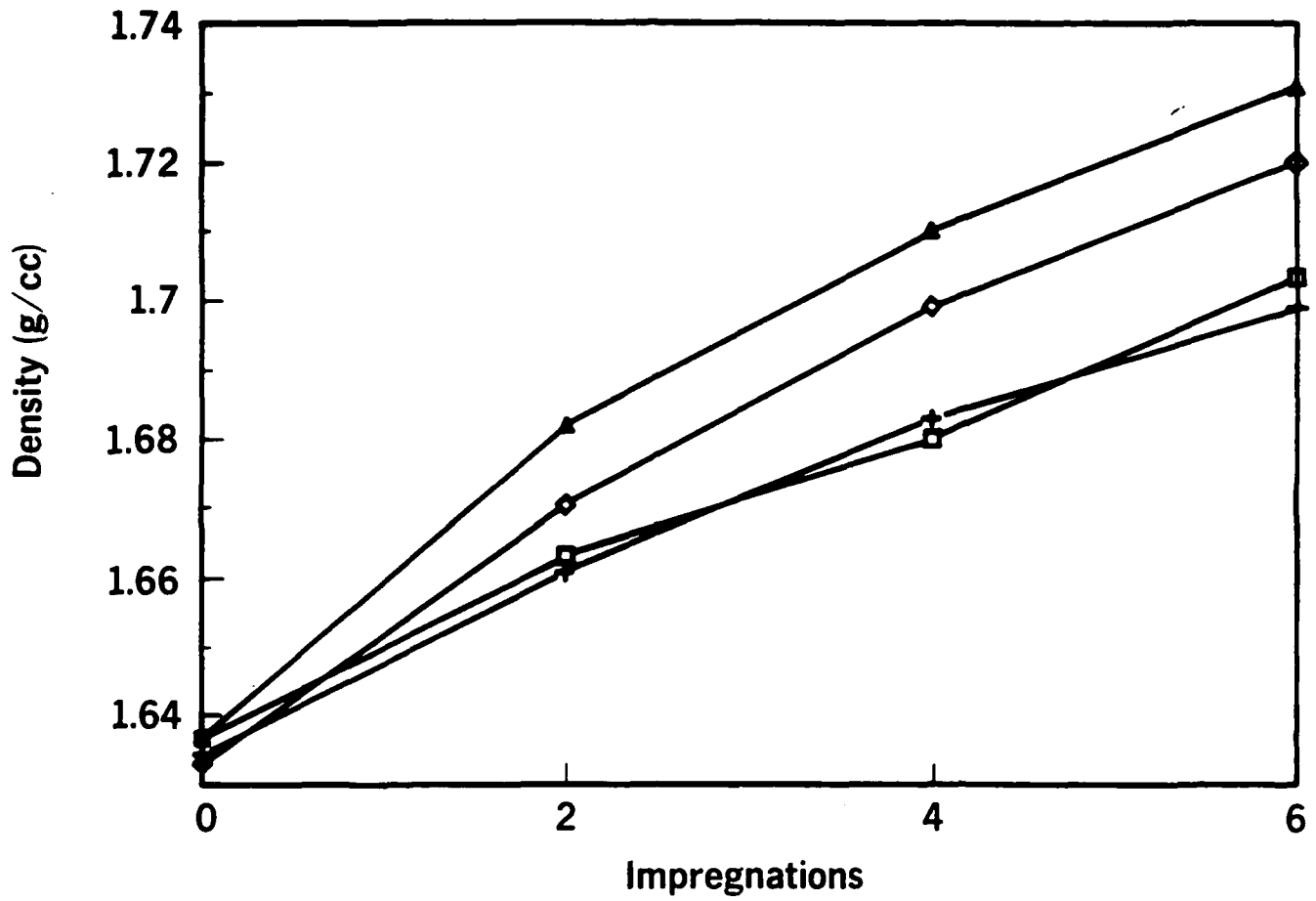


FIGURE 18 ACC2 IMPREGNATION DENSITY CHANGE

# Porosity Change

ACC2 (1000C)

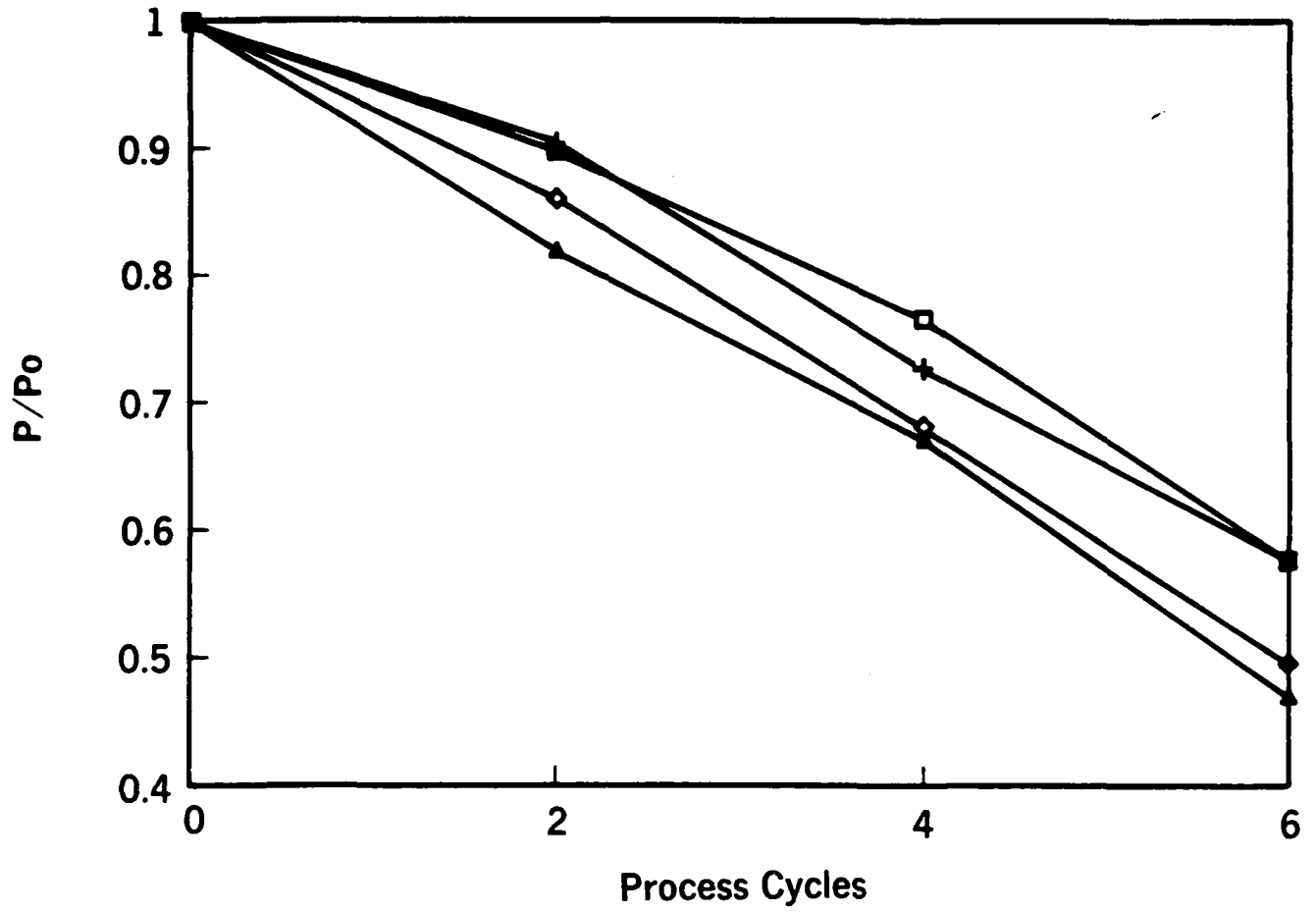


FIGURE 19 ACC2 IMPREGNATION POROSITY CHANGE



Figure 20 illustrates the bulk density change as a function of impregnation for a high density 3D carbon/carbon sample. As expected, the low initial porosity (about 4 percent) resulted in a smaller density increase than for the ACC2 samples discussed above. The 3-D samples were included for comparison with 2-D material because their significantly lower porosity would provide a more difficult microstructure to penetrate.

#### 4.5 FIBER COATING RESULTS

Recent discussions regarding thermal stability limitations of ceramic fibers prompted a series of experiments designed to use SCF processing to coat Nextel 440 fibers with polycarbosilane. Tests were conducted with PCS (parent polymer), PCS-1000 (the lowest molecular weight fraction), and PCS+3000 (a high molecular weight fraction). Figure 21 illustrates the resulting microstructures of the following pyrolyzed samples:

- A. PCS-1000
- B. PCS
- C. PCS+3000

These micrographs show that continuous coatings were achieved for all fractions. Polymer accumulations noted at fiber contact points were probably caused by the surface tension of the precipitated liquid phase.

The continuous coatings produced on the fiber tape preforms suggested that this might be a useful initial and final coating process for carbon/carbon composites. Considering the dilute concentration of polymer in supercritical propane used in this methods, maximum penetration should be possible without the problems associated with high molecular weight surface coatings that could be present at normal polymer concentrations. In addition, thin coatings exhibit very little cracking and would provide increased resistance to oxidation. As a final coating, SCF-derived thin films would be able to penetrate CVD surface coating cracks and further enhance oxidation resistance.

# 3D Carbon/Carbon Density Change

530 T2 Z2

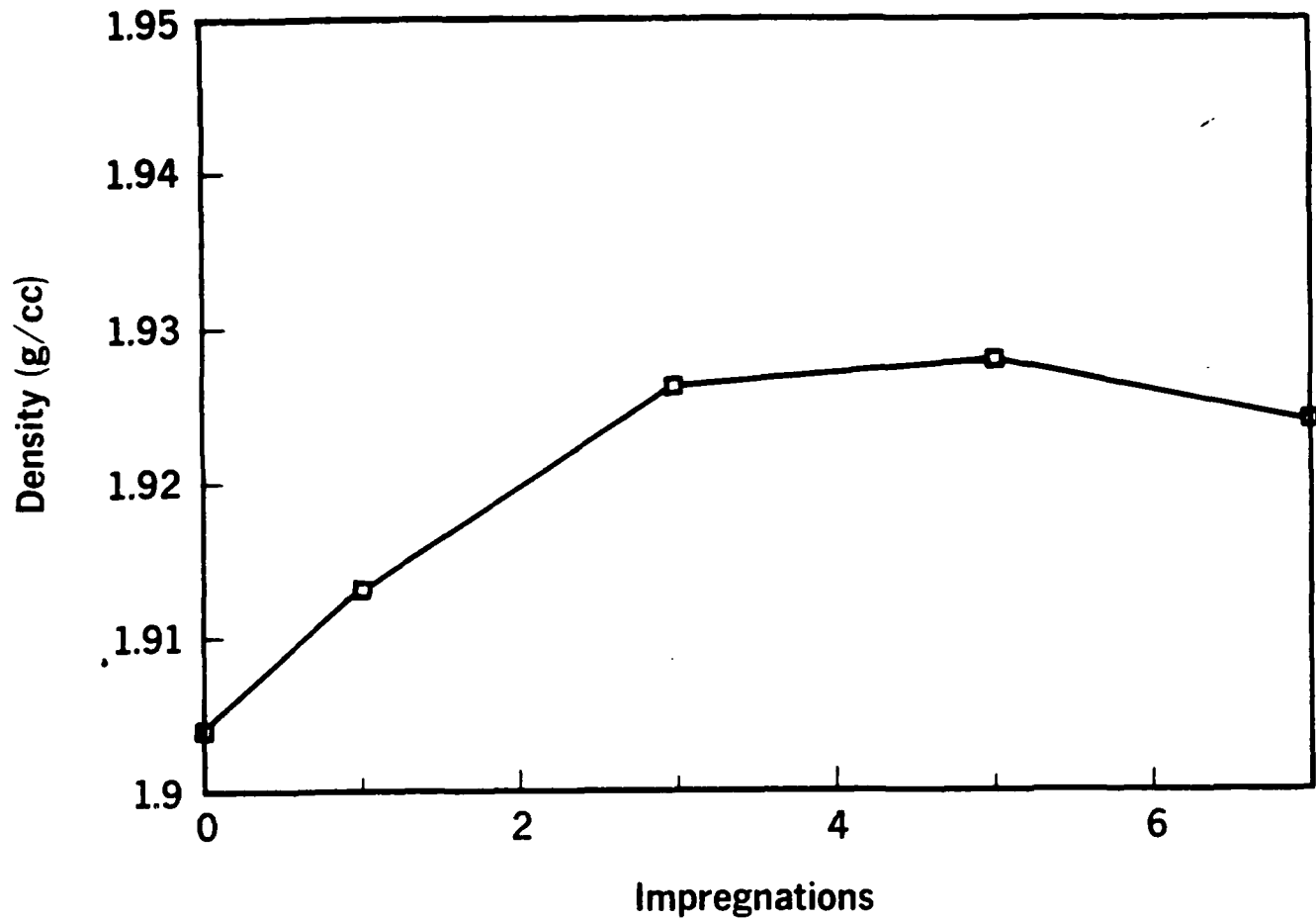
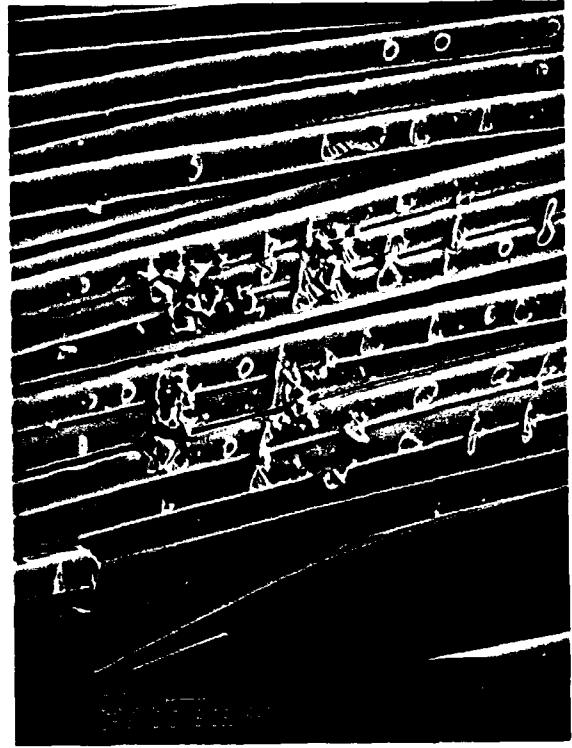


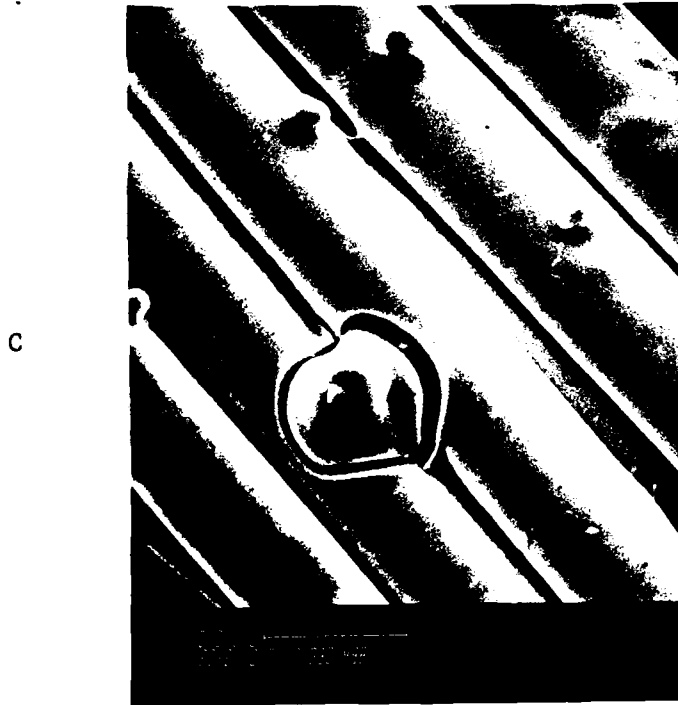
FIGURE 20 3D CARBON/CARBON DENSITY CHANGE



A



B



C

FIGURE 21 SCF FIBER COATING MICROSTRUCTURE

#### 4.6 MECHANICAL PROPERTIES

Three point flexural strength of ACC2 increased from 197 MPa for the as received material to 291 MPa for samples impregnated six times. Test samples measuring 3 mm x 13 mm x 75 mm were tested on a 63 mm span. All samples failed in a non-brittle fashion by buckling of the compression side of the sample.

#### 4.7 OXIDATION PROPERTIES

Oxidation resistance was measured at 510°C, 538°C, and 593°C by comparing the weight loss as a function of time of SCF impregnated and as received ACC2 samples.

Figure 22 illustrates the relative oxidation resistance at 510°C in air. After seven hours, the as received sample lost about five percent of its original weight compared to a 0.25 percent weight loss for the SCF impregnated sample.

At 538°C, an alternate impregnation method using a liquid polycarbosilane/toluene solution was compared to as received and SCF impregnated samples as shown in Figure 23. The liquid impregnated samples also received six impregnation/pyrolysis cycles but the resulting oxidation resistance was less than that exhibited by the SCF processed samples.

Figure 24 compares the 593°C oxidation resistance of as received and SCF impregnated samples. The data shown on this figure were obtained from the stressed oxidation test described in the next section.

The effect of oxidation on the structural integrity of as received and SCF impregnated samples was determined by measuring the deflection of three point bend samples as a function of time at 593°C as shown in Figure 25. The applied stress was 69 MPa and the number of each curve indicates the number of SCF impregnations given that sample. The increased load bearing resistance with increasing impregnation cycles is apparent and provides a useful demonstration of the effectiveness of the SCF process.

# 510C Oxidation Results

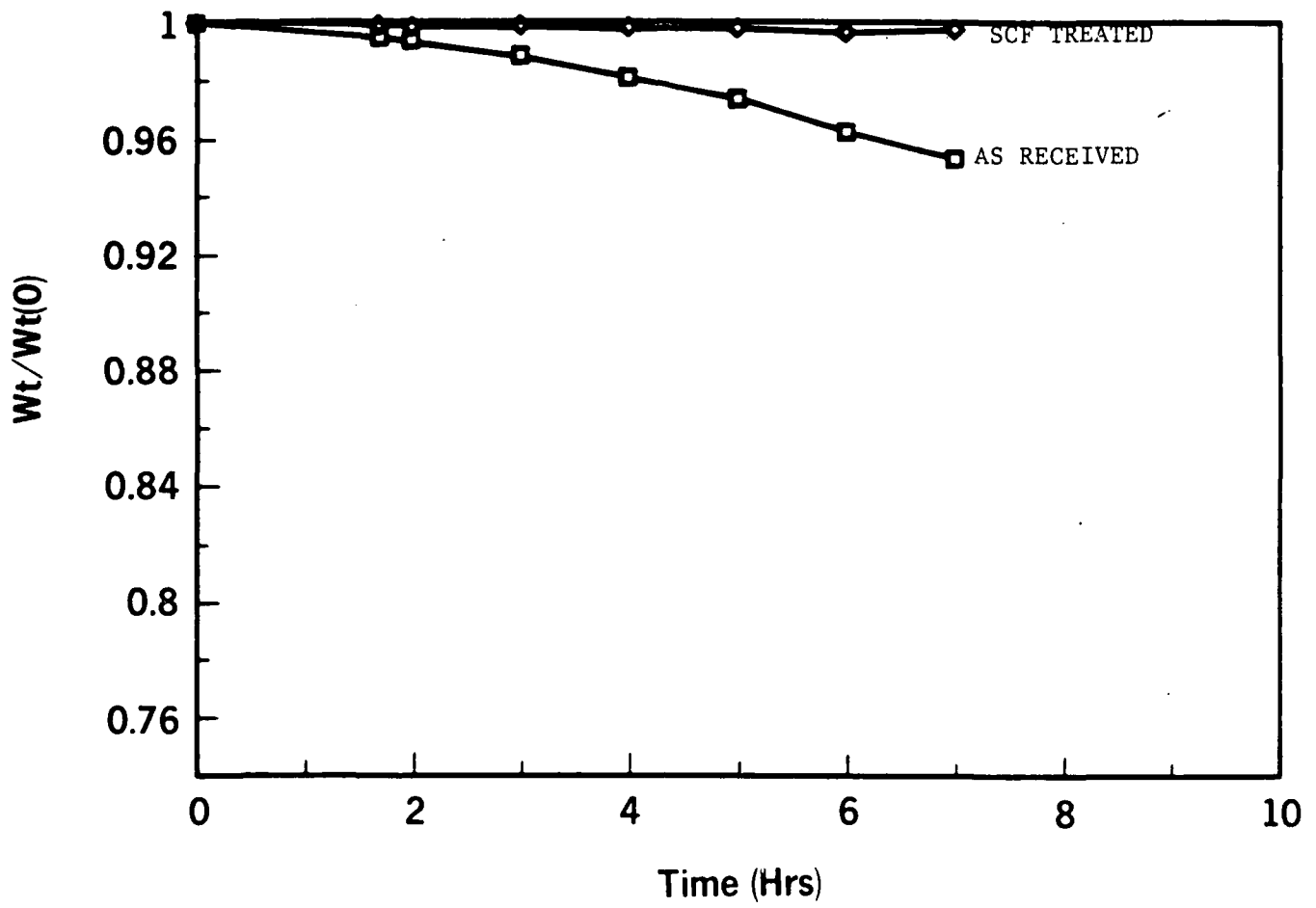


FIGURE 22 510°C OXIDATION RESULTS

# 538C Oxidation Weight Loss

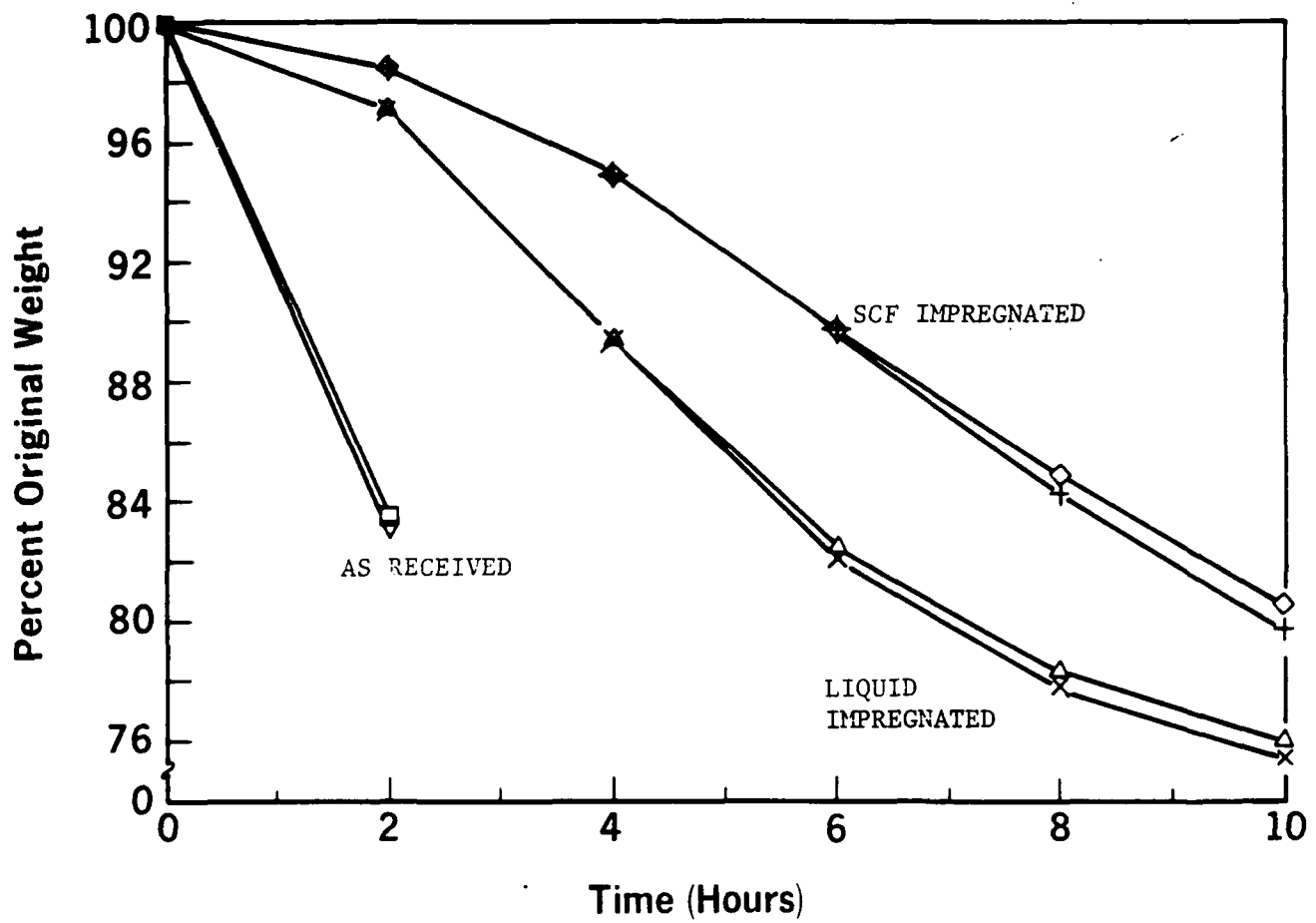


FIGURE 23 538°C OXIDATION WEIGHT LOSS

# 593C Oxidation Results

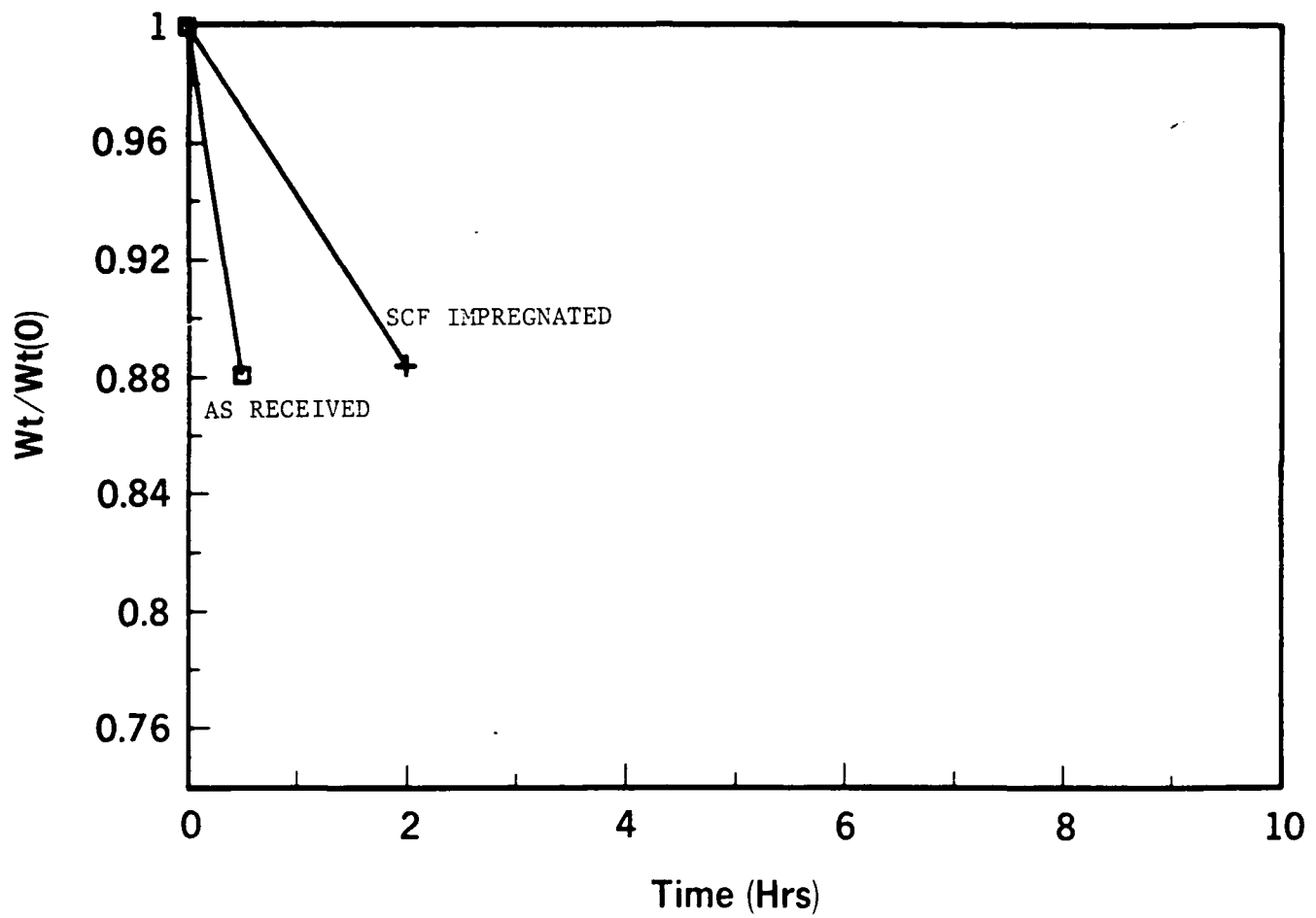


FIGURE 24 593°C OXIDATION RESULTS

# Stressed Oxidation

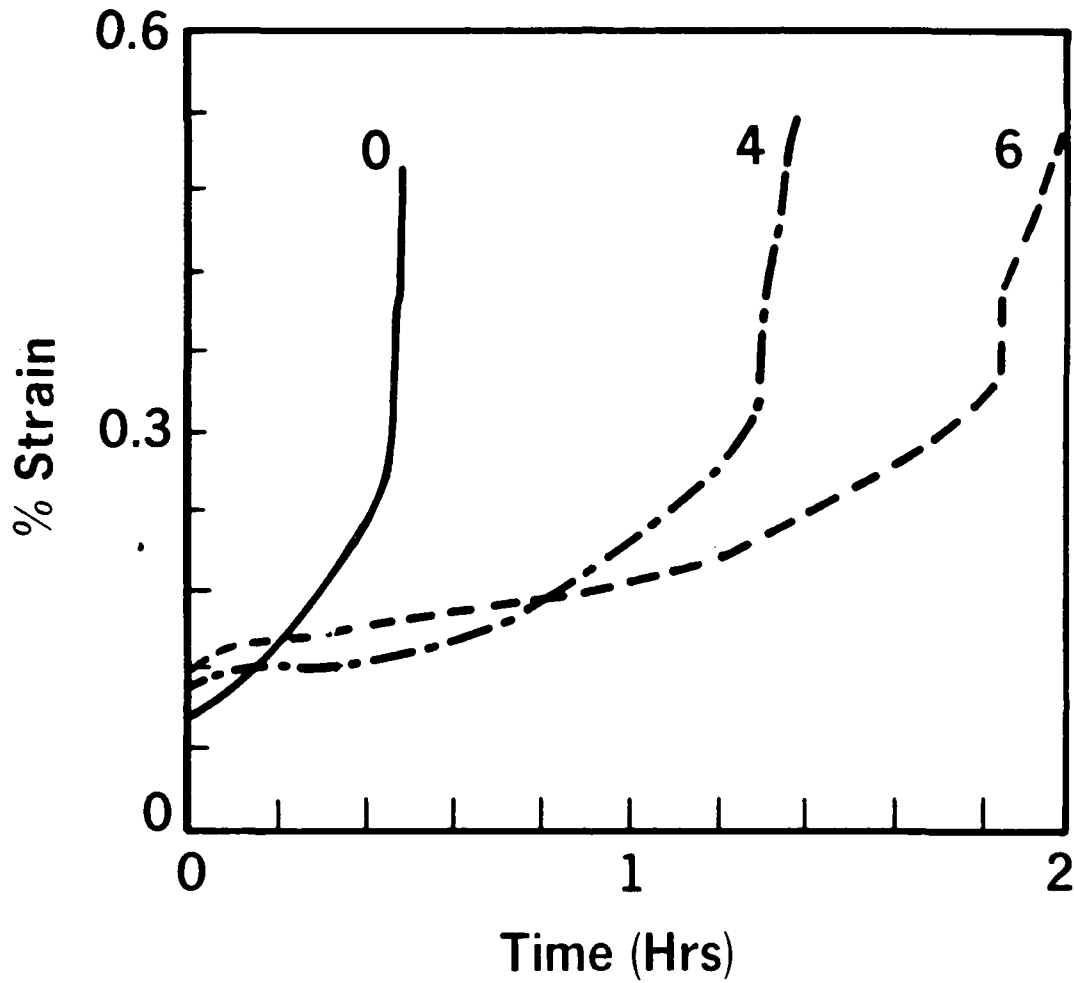


FIGURE 25 593°C STRESSED OXIDATION RESULTS



Oxidation resistance results are summarized in Figure 26, a plot of the log of the initial oxidation rate in ( $\text{Kg}/\text{M}^2 \text{ sec}$ ) versus temperature. It is apparent that significantly improved oxidation resistance in the temperature range of 500 to 600°C resulted from the SCF impregnation process.

#### 4.8 MICROSTRUCTURE

The silicon distribution was considered the key to the correlation between structure and properties. Analysis of polished sections by back scattered electron (BSE) imaging and silicon dot mapping provided a detailed picture of sample microstructure.

Silicon distributions in as received and SCF impregnated ACC2 are compared in the BSE and silicon dot map image pairs shown in Figure 27. As expected, only background noise was detected in the silicon dot map of the as received sample, Figure 27B. Distinct patterns of silicon concentrations corresponding to substrate cracks are very apparent throughout the cross section of the SCF impregnated sample as shown in Figure 27D.

Figure 28 gives a more detailed image of silicon depositions in ACC2. Silicon accumulations along cracks or low density regions parallel to the fibers are believed to be responsible for the increased oxidation resistance of these samples.

The BSE and silicon dot map image pair shown in Figure 29A and B of a polished section in the plane of the composite illustrates the silicon distribution at fiber weave intersections. The silicon dot map also shows silicon concentrations along fibers throughout the image area. Figure 29 is a BSE image showing the excellent penetration of polymer along the fiber/matrix interface.

A similar microstructural analysis is shown in Figures 30, 31, and 32 for a high density 3-D sample. As discussed above, the apparent porosity of this sample was four percent prior to impregnation. Fiber architecture and general silicon distribution are shown in the BSE and silicon dot map pair in Figure 30.

# Oxidation Rate of ACC2

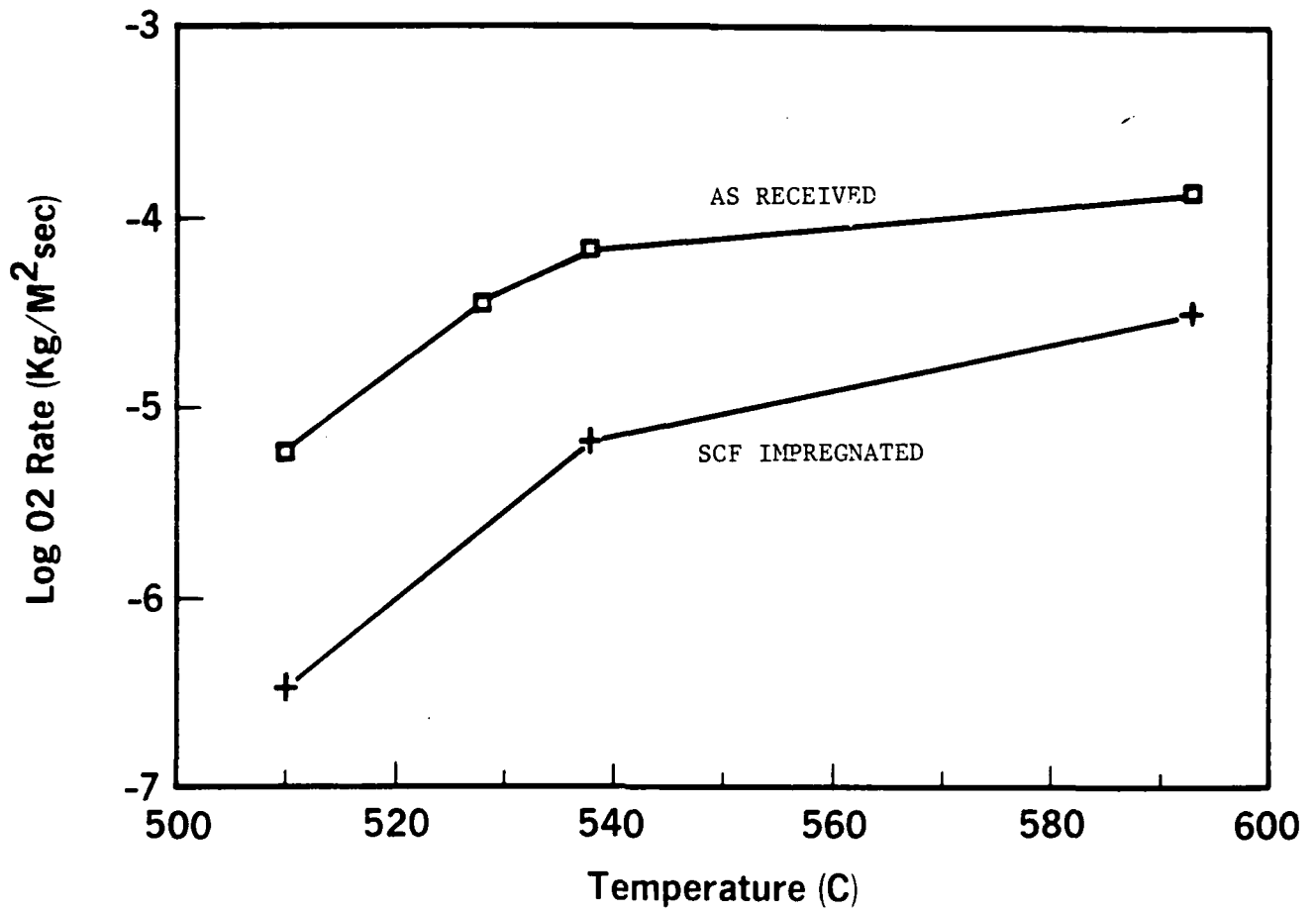
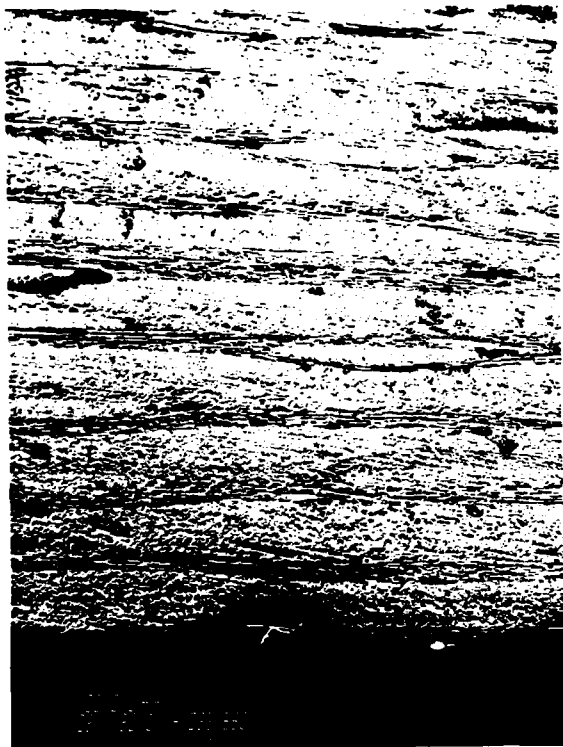
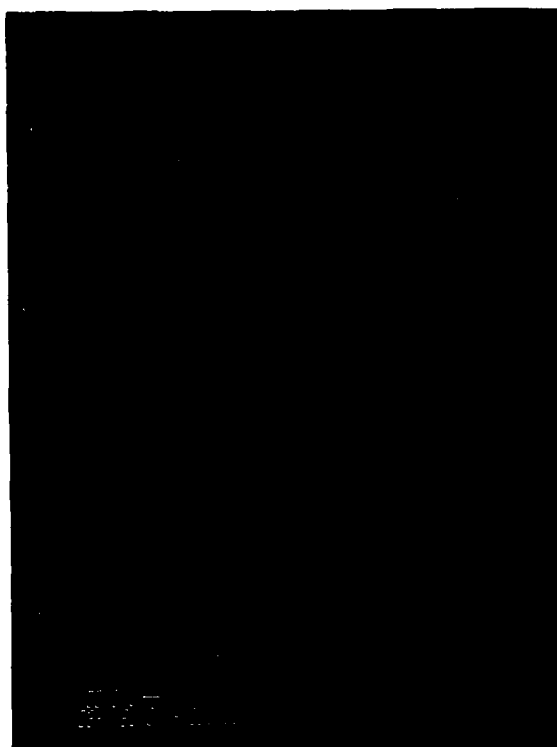


FIGURE 26 Oxidation Rate of as Received and SCF Impregnated ACC2



A



B

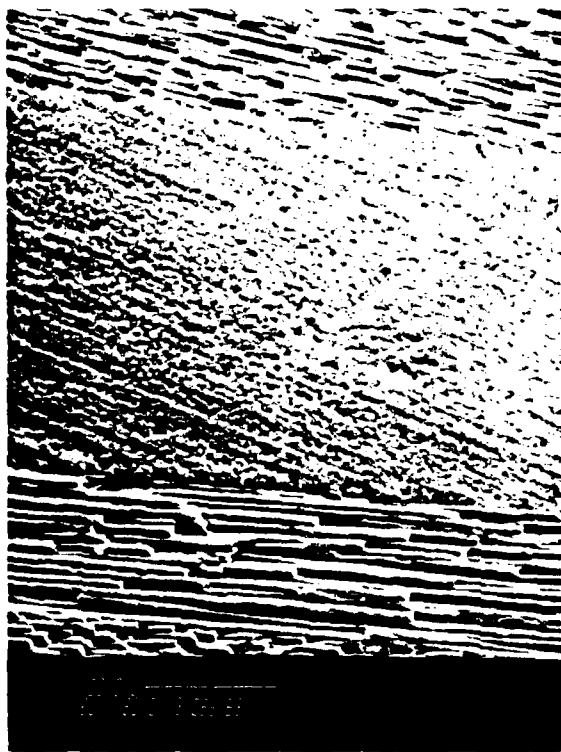


C

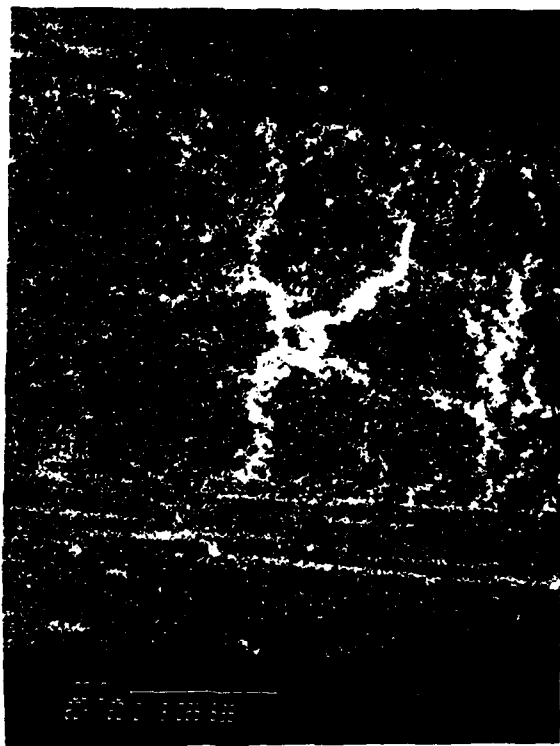


D

FIGURE 27 AS RECEIVED AND SCF IMPREGNATED ACC2  
MICROSTRUCTURES

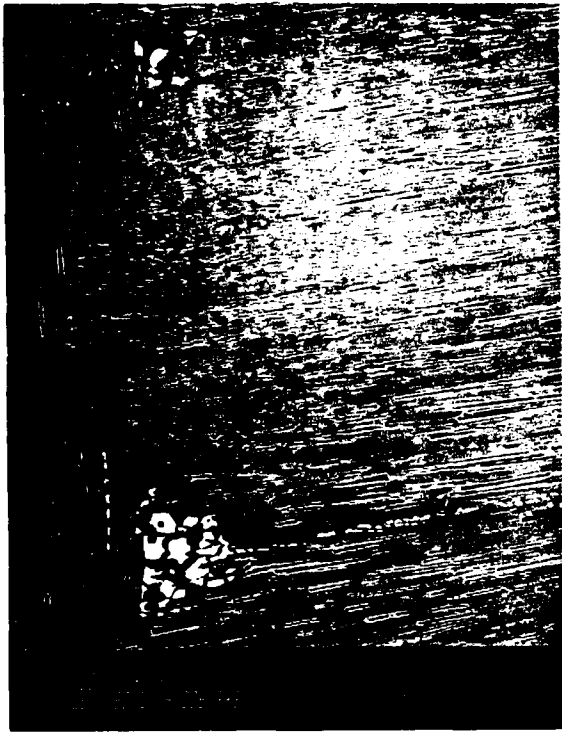


A

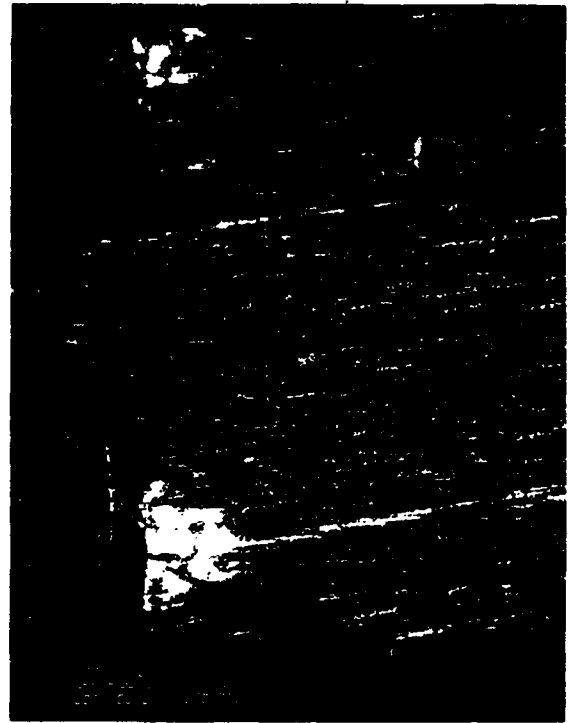


B

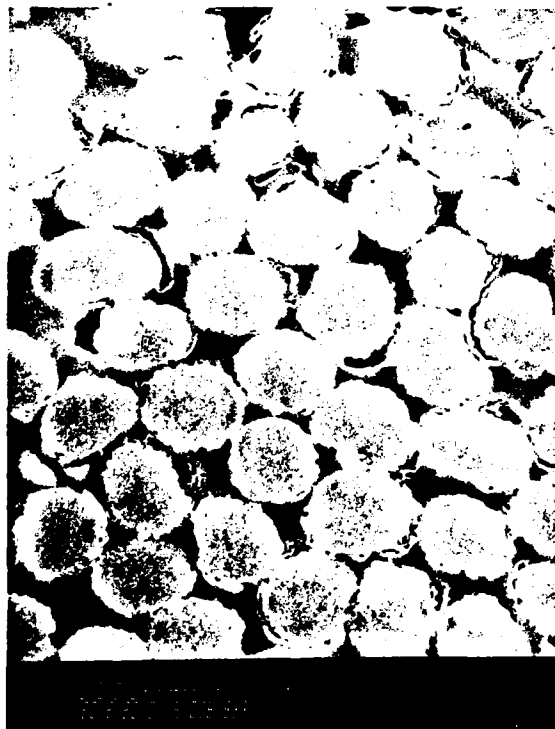
FIGURE 28 SiC CONCENTRATION IN ACC2



A

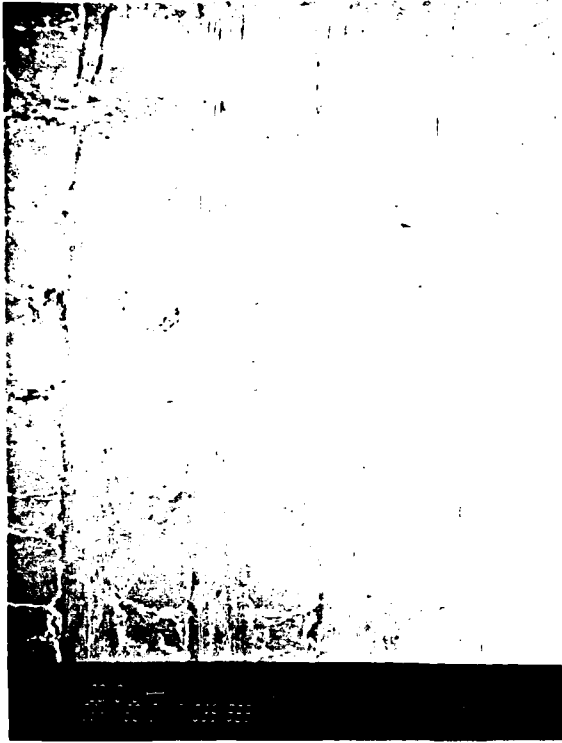


B

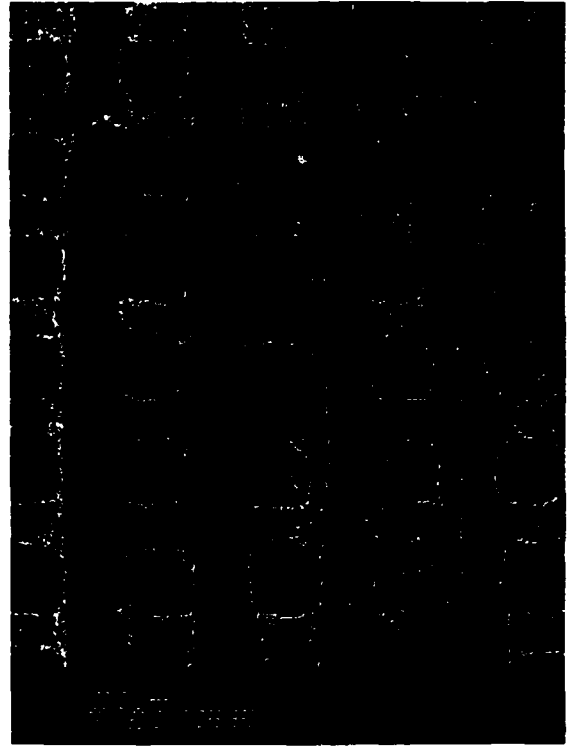


C

FIGURE 29 SIC FILLED WEAVE INTERSECTIONS AND FIBER/MATRIX INTERFACE IN ACC2



A



B

FIGURE 30 CROSS SECTION OF SCF IMPREGNATED 3D C/C



A



B

FIGURE 31 S1C ACCUMULATION AT TOW BUNDLE INTERFACE

The silicon concentration between the tow bundle and matrix is shown in greater detail in the secondary electron and BSE image pair of Figure 31. Quite effective filling of the gap between the tow and matrix is apparent.

Figure 32 illustrates the silicon distribution in a small crack within a tow bundle. This secondary electron and BSE image pair reveals a dense accumulation of silicon in the gap between fibers and matrix. This ability to fill and/or coat potential oxygen paths with oxidation resistant material contributed to the observed oxidation property improvements.

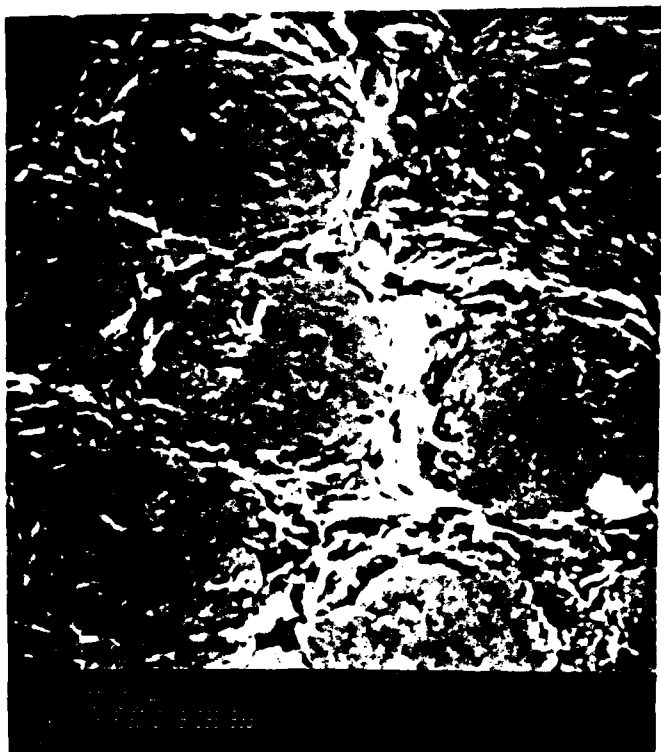
#### 5.0 CONCLUSIONS

Supercritical fluids were successfully utilized to impregnate and densify a variety of carbon/carbon composites with polycarbosilane. As a result of this process, significant improvements in oxidation resistance and mechanical properties were observed. In addition, SCF refinement of preceramic polymers resulted in increased insitu char yields and hence more efficient processing. Finally, dilute SCF solutions were used to apply continuous coatings on NEXTEL fibers.

#### 6.0 RECOMMENDATIONS

The utility of SCF processing to enhance the oxidation resistance of carbon/carbon composites has been demonstrated. This approach should be extended to develop multicomponent glass forming systems which will result in more effective sealing of coating cracks and substrate porosity. Furthermore, a better understanding of the interactions of SCF derived matrix inhibition systems with current coatings is required. Additional work is also necessary to control fiber/matrix interactions through the application of SCF fiber coatings.





A



B

FIGURE 32 SiC FILLED TOW BUNDLE CRACK

## REFERENCES

1. Price, R. J., P. E. Gray, G. B. Engle, J. E. Sheehan, "Advanced Oxidation-Inhibited Matrix Systems for Structural Carbon/Carbon Composites", June 1987, AFWAL-TR-87-4042.
2. Eitman, D. A., W. C. Loomis, "Advanced Oxidation Protection Systems for Structural Carbon/Carbon Composites", September 1986, AFWAL-TR-86-4069.
3. M. McHugh and V. J. Krukonis, Supercritical Fluid Extraction (Butterworths Publishers, Boston, 1986), p. 69-78.
4. L. G. Randall, Separation Science and Technology, 17(1), p. 1-118, 1982.
5. D. F. Williams, Chemical Engineering Science, 36(11) p. 1769-1788, 1981.
6. Hannay, J. B., and H. Hogarth, J. Proc. Roy. Soc. London, 29, 324 (1879).
7. D. B. Todd and J. L. Elgin, AICHE Jour., 1, 20 (1955).
8. C. L. Schilling, Jr., "Organosilam Polymers, VII: Sodium Derived Vinylic Polysilanes", ONR Technical Report 83-3, September 1983.
9. S. Yajima, "Special Heat-Resisting Materials from Organometallic Polymers", Am. Ceram. Soc. Bull. 62(8) P. 893-898, 1983.